

AD-A075 131

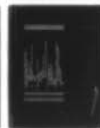
NAVAL OCEAN SYSTEMS CENTER SAN DIEGO CA  
PHASE INTEGRAL ALGORITHMS FOR SIGNAL SPEEDS IN RANGE-DEPENDENT --ETC(U)  
JUL 78 R C SHOCKLEY  
NOSC/TR-412

F/G 17/1

UNCLASSIFIED

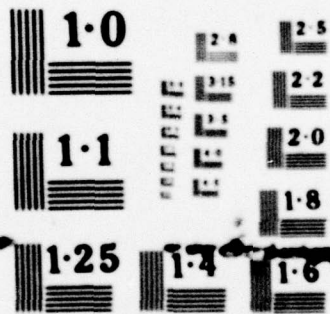
NL

1 OF 1  
AD-  
A075131



END  
DATE  
FILMED  
11-79  
DDC





NATIONAL BUREAU OF STANDARDS  
MICROCOPY RESOLUTION TEST CHART

AD A075131

# NOSC

NOSC TR 412

LEVEL II

NOSC TR 412

Technical Report 412

## PHASE INTEGRAL ALGORITHMS FOR SIGNAL SPEEDS IN RANGE-DEPENDENT SOUND VELOCITY PROFILES

R. C. Shockley

10 July 1978

Final Report: January 1978 — July 1978

Prepared for  
Naval Electronic Systems Command  
(PME 124)

DDC FILE COPY

Approved for public release; distribution unlimited

DDC  
RECEIVED  
OCT 17 1978  
A

NAVAL OCEAN SYSTEMS CENTER  
SAN DIEGO, CALIFORNIA 92152

79 10 17 069



NAVAL OCEAN SYSTEMS CENTER, SAN DIEGO, CA 92162

---

AN ACTIVITY OF THE NAVAL MATERIAL COMMAND

**RR GAVAZZI, CAPT, USN**

Commander

**HL BLOOD**

Technical Director

#### ADMINISTRATIVE INFORMATION

This work pertains to a method for estimating from archival sound speed profile data the effective signal speed in range-dependent environments. The method employs the adiabatic invariance of the phase integral for underwater sound rays, and offers certain computational advantages in the context of improved time-difference-of-arrival performance using Multi-Array Correlation (MAC) equipment. The work was done under NOSC 24311N, X0522114, and was sponsored by Naval Electronic Systems Command (PME-124).

Released by  
M. R. Akers, Head  
System Concepts and Analysis Division

Under Authority of  
E. B. Tunstall, Head  
Ocean Surveillance Department

UNCLASSIFIED

SECURITY CLASSIFICATION OF THIS PAGE (When Data Entered)

REPORT DOCUMENTATION PAGE		READ INSTRUCTIONS BEFORE COMPLETING FORM
1. REPORT NUMBER Technical Report 412 (TR 412)	2. GOVT ACCESSION NO. 14	3. RECIPIENT'S CATALOG NUMBER NOSC/TR-412
4. TITLE (and Subtitle) PHASE INTEGRAL ALGORITHMS FOR SIGNAL SPEEDS IN RANGE-DEPENDENT SOUND VELOCITY PROFILES	5. TYPE OF REPORT & PERIOD COVERED Final Report Jan 1978 - Jul 1978	6. PERFORMING ORG. REPORT NUMBER
		7. AUTHOR R. C. Shockley
8. PERFORMING ORGANIZATION NAME AND ADDRESS Naval Ocean Systems Center San Diego, CA 92110	9. PROGRAM ELEMENT, PROJECT, TASK AREA & WORK UNIT NUMBERS 24311N XO522114	
11. CONTROLLING OFFICE NAME AND ADDRESS Naval Electronic Systems Command Washington, DC 20360	12. REPORT DATE 18 Jul 1978	13. NUMBER OF PAGES 47
	14. MONITORING AGENCY NAME & ADDRESS (if different from Controlling Office)	15. SECURITY CLASS. (of this report) Unclassified
16. DISTRIBUTION STATEMENT (of this Report)  Approved for public release; distribution unlimited.		15a. DECLASSIFICATION/DOWNGRADING SCHEDULE
17. DISTRIBUTION STATEMENT (of the abstract entered in Block 20, if different from Report)		
18. SUPPLEMENTARY NOTES		
19. KEY WORDS (Continue on reverse side if necessary and identify by block number) Adiabatic invariant                      Sound speed algorithms Guided propagation                      Underwater sound Range dependent profiles SOFAR		
20. ABSTRACT (Continue on reverse side if necessary and identify by block number) The adiabatic invariance of the phase integral $J = \oint \sin \theta dz/c$ for ducted sound rays in SOFAR channels is demonstrated by means of exact raytracing solutions in range-dependent channels. FORTRAN algorithms for this and for relating $J$ to the average ray speed in arbitrary ducts are presented and discussed in the context of acoustic surveillance.		

DD FORM 1 JAN 73 1473

EDITION OF 1 NOV 68 IS OBSOLETE  
S/N 0102-LF-014-6601

UNCLASSIFIED

SECURITY CLASSIFICATION OF THIS PAGE (When Data Entered)

393 159

## FOREWORD

This report presents two Fortran raytracing codes and related theory which are designed to treat underwater sound propagation in the presence of range-dependent sound velocity profiles (SVPs). Particular emphasis is placed on the average horizontal ray velocity and its variation as a ray traverses different SVPs. Efficient calculation of this variation is of great importance for improved modern multisensor localization techniques. The following pages discuss the adiabatic invariant approximation (AIA) and the use of the codes RAY1 and RAY2 in sufficient depth that the reader may apply them to his own problems or modify them for this purpose. This work was supported by the Naval Electronic Systems Command PME-124 under the Performance Evaluation and Prediction program at the Naval Ocean Systems Center. Portions of this work have appeared in the Journal of the Acoustical Society of America.

## OBJECTIVE

The objective of the work was to calculate efficiently the variation of the average horizontal ray velocity as the ray traverses different sound velocity profiles. Efficient calculation of this variation is of great importance for improved modern multisensor localization techniques.

## RESULTS

The adiabatic invariant approximation agrees well with exact raytracing results even for strongly inhomogeneous sound velocity profiles. Simple algorithms are developed for demonstrating this and for computing the adiabatic invariant in arbitrary profiles for a user-selected family of rays.

## RECOMMENDATIONS

A set of curves or tables should be prepared showing the functional relation between the adiabatic invariant, the average sound speed, and the ray angle, for areas of high interest in acoustic surveillance. These would provide a data base for improved multisensor localization and would reduce the calculation of average ray speeds to a table-look-up procedure once the location of the source is known approximately.

Accession For	
NTIS GRA&I	<input checked="" type="checkbox"/>
DDC TAB	<input type="checkbox"/>
Unannounced	<input type="checkbox"/>
Justification	<input type="checkbox"/>
By _____	
Distribution/	
Availability Codes	
Disc	Avail and/or special
A	

## CONTENTS

I. INTRODUCTION . . .	page 3
II. GENERAL DESCRIPTION OF RAY1 AND RAY2 . . .	4
A. The Adiabatic Invariant for Sound Rays . . .	4
B. General Description of RAY1 . . .	8
C. General Description of RAY2 . . .	12
III. INSTRUCTIONS FOR USING RAY1 . . .	15
A. Input Requirements . . .	15
B. Output . . .	15
IV. INSTRUCTIONS FOR USING RAY2 . . .	17
A. Input Parameter List . . .	17
B. Output . . .	18
V. INTERNAL LOGICAL STRUCTURE OF RAY1 AND RAY2 . . .	20
A. Internal Structure of RAY1 . . .	20
B. Internal Structure of RAY2 . . .	22
VI. LISTINGS OF RAY1 AND RAY2 . . .	24
REFERENCES . . .	47

## I. INTRODUCTION

Several important problems in underwater sound, ionospheric propagation, and seismic research involve the presence of ducts or waveguides which effectively trap the energy, greatly reducing transmission loss over the corresponding case of an isotropic medium. Often, however, the duct varies with range, precluding exact normal mode solutions and affecting signal speeds in a generally complicated fashion. The range variation may consist of changes in the physical dimensions of the duct or in the index of refraction across the duct.

Simple computational methods are desired for estimating the influence of such range-dependence. The requirements basically are that the procedure be readily checked against known exact solutions, that it be relatively inexpensive to implement using archival data bases, and that revisions of the data should be readily incorporated in the method, without requiring massive recomputation.

An attractive candidate for meeting these needs is the adiabatic invariant approximation (AIA). This presupposes that in the cases of interest any range-dependent variations take place over distances large compared to a single ray cycle. In other words, the properties of the medium should be sensibly constant over a cycle. Under such conditions, which nearly always apply for deep sound channels, it turns out that ray paths evolve in range so as to keep a certain quantity ( $J$ ) constant, known as the action integral or phase integral.<sup>1</sup> This "conservation law" allows one to follow a ray, in essence, without ever tracing it over its entire path. It is only necessary to know in each local region how the quantities of interest (eg. maximum depth of the ray, vertexing speed, average horizontal velocity, etc.) are related to the adiabatic invariant  $J$ , something easily done simply by tracing a few ray cycles in each local region.

Although we have been speaking in terms of rays, adiabatic invariants appear in mode theory as well. Each mode corresponds to a particular vertexing depth and speed for the associated family of rays. In referring only to rays, as we shall do throughout what follows, we are assuming the duct supports so many modes that they comprise a continuum in effect; their discrete nature may be disregarded without significant loss of accuracy. Since deep sound channels are of the order of ten or more wavelengths across at frequencies of interest for time difference fixing, the mode-continuum approximation is generally quite good. The low order modes are not strongly excited by acoustic sources, which are usually far from the sound channel axis.

When one has only low order modes, the adiabatic invariants are the mode numbers themselves. This is intuitively plausible, for if one considers an arbitrarily gradual evolution of one duct into a second one, having, say, a somewhat different index profile, then it is clear that the power initially in a particular mode must equal the power in that mode in the altered duct. Only rather strong perturbations will cause mode coupling; in their absence, there is no cause for energy to distribute itself among any other discrete modes.

---

1. Weston, DE, *Guided Propagation in a Slowly Varying Medium*, Proc. Phys. Soc. (London) v. 73, p. 365-384, 1958.

Exceptions to this simple picture obviously exist in cases where one duct evolves into two. In such cases one cannot treat the splitting of acoustic energy accurately unless the details of the SVP evolution are considered. Fortunately, such cases are rare. The procedures described in this report should be applicable to all ocean areas of surveillance interest.

The computer codes described here serve two purposes. RAY1 allows one to set up a radically inhomogeneous medium whose SVP has a prescribed functional form and to determine numerically by how much the approximation  $J = \text{constant}$  fails for various horizontal gradients. RAY2 allows one to input an arbitrary but range-independent SVP and to trace a family of rays in order to find the relation between  $J$  and other properties of interest for rays in that particular SVP. The former code is of primarily theoretical interest, and serves to establish the accuracy for the AIA in analytically tractable cases, while it is our hope that the latter will serve as a model for implementation of AIA methods in acoustic surveillance.

In section II we describe in general terms the scope of RAY1 and RAY2, we review briefly the adiabatic invariant theory as applied to acoustic rays, the analogous problem in classical mechanics, and finally give the AIA signal speed algorithm. Sections III and IV provide instructions in detail on the procedure for executing RAY1 and RAY2. In section V, we shall treat the internal logical structure of RAY1 and RAY2 in order to pave the way for any changes deemed necessary or desirable. Listings of the Fortran source code appear in section VI.

## II. GENERAL DESCRIPTION OF RAY1 AND RAY2

In this section we shall describe the general features of RAY1 and RAY2 and the theory behind these codes. In sections III and IV we shall present specific information needed to make runs with these codes. Here we are concerned with the practical need for such codes, and the underlying concept of using an adiabatic invariant as a means for following the evolution of rays in range-dependent SVPs.

### A. THE ADIABATIC INVARIANT FOR SOUND RAYS

The basic problem of time-difference fixing provides a context for introducing the adiabatic invariant concept. For simplicity, suppose that acoustic signals propagate with the same speed in the ocean regardless of direction. In this isotropic ocean, a pair of sensors which receive a given signal may determine, based on the difference of arrival times, a locus of points on which the source must lie. The locus is a hyperbola with the sensors as foci. If  $R_1$  and  $R_2$  represent distances to sensors 1 and 2 respectively, and  $c\Delta t$  represents the equivalent delay length, then  $|R_1 - R_2| = c\Delta t$  determines the hyperbola. A third sensor, or some additional data from one of the original two, then suffices to locate the source uniquely. (Ambiguities arising in particular geometries are not of interest here, although they may be important in practice.)

The procedure just described works only approximately in actual ocean environments. For long-range detections on the order of several hundred kilometers the signal speed generally will vary with range. Modern acoustic surveillance systems are capable of sufficiently precise measurement that this inhomogeneity poses a major limitation on localization. How can one determine an appropriate average sound speed so as to construct the needed locus?

A natural solution is to use a conserved quantity for sound rays in range-dependent environments. Weston<sup>1</sup> has pointed out that the quantity

$$J = \oint c^{-1} \sin\theta \, dz \quad (1)$$

is conserved provided that changes in the SVP are sufficiently gradual, or "adiabatic." Here  $c$  is the local depth-dependent sound speed, and is regarded as being range-independent over the period of integration (one ray cycle),  $\theta$  is the ray angle measured with respect to horizontal, and  $z$  is the depth coordinate (usually taken as positive downwards). More detailed discussion of the invariance of  $J$  in range-dependent SVPs, as well as a short bibliography on the topic, will be found in reference 2. A proof of the adiabatic invariance of the action integral will be found in reference 3. At this point it may be of interest to consider the mechanical analogue of trapped sound rays and eq (1).

### 1. Classical Mechanical Analogy

Ray theory is of course an approximation to an "exact" wave theory of propagation. In the same sense, classical mechanics is an approximation to the more precise quantum mechanical theory. In both cases the smallness of the wavelength with respect to the physical dimensions of the medium or measuring apparatus involved permits one to pass over to the geometrical optics limit, ignoring small wavelength-dependent corrections. In classical mechanics, the motion of a system is obtainable from Hamilton's principle, which is a variational principle, stating that the actual trajectory followed is such as to minimize the integral  $\int_{t_1}^{t_2} L(\dot{q}, q; t) \, dt$ . (Actually the statement of Hamilton's principle permits maximization as well, but we shall not be concerned with this in what follows.) Here  $L$  is the Lagrangian, a function of the coordinates and velocities, symbolically denoted  $q$  and  $\dot{q}$ , respectively, and possibly of time  $t$ . The coordinates and velocities are functions of time. The system moves from some fixed starting point  $(q(t_1), \dot{q}(t_1))$  to a final point  $(q(t_2), \dot{q}(t_2))$ , also fixed. Hamilton's principle is written

$$\delta \int_{t_1}^{t_2} L \, dt = 0 \quad (2)$$

where  $\delta$  indicates an infinitesimal variation of the path. Equation (2) states that the system follows a minimizing trajectory, since any infinitesimal variation about the trajectory must produce no change in the value of the integral.

In classical mechanics, the equations of motion follow if one uses for the Lagrangian  $L = T - V$ , where  $T$  is the kinetic energy and  $V$  the potential energy of the system. Then the calculus of variations yields, as a theorem from eq (2), Newton's equation of motion.

2. Shockley, RC, *Paraxial and Nonparaxial Ray Speeds in Strongly Range-Dependent SOFAR Channels*, J. Acoust. Soc. Am. v. 64, p. 1171-1177 (1978).

3. Landau, LD and Lifshitz, EM, *Mechanics*, Pergamon Press, Reading, Mass., p. 154-158, 1960.

Variational principles (with different choices for  $L$ ) also lead to the equations of electrodynamics, hydrodynamics, quantum mechanics, etc., in similar fashion.

If we consider Fermat's principle, the similarity to Hamilton's principle is clear. Fermat's principle states that a ray will follow that trajectory minimizing the time of flight between a given initial and final point:

$$\delta \int_1^2 dt = \delta \int_1^2 ds/c = 0 \quad (3)$$

where  $ds$  is an infinitesimal element of length along the ray path and  $c$  the speed of propagation in the medium.

For concreteness, we restrict our discussion to a slab symmetric medium and let  $x$  be the horizontal and  $z$  the vertical coordinate. Then eq (3) becomes

$$\delta \int_1^2 c^{-1} (1 + \dot{z}^2)^{1/2} dx = 0 \quad (4)$$

where  $\dot{z} \equiv dz/dx$  is the slope of the ray. This result now is identical to eq (2), Hamilton's principle, under the transformation

$$\begin{aligned} t &\rightarrow x, \\ q &\rightarrow z, \\ L(q, \dot{q}; t) &\rightarrow (1 + \dot{z}^2)^{1/2}/c(z; x). \end{aligned} \quad (5)$$

Thus range plays the role of time in the mechanical problem, and the depth  $z$  is analogous to particle displacement. Hence  $\dot{z} = \tan\theta$  is analogous to velocity. Note that  $L$  does not resemble a quantity like  $T-V$ .

It is natural to ask what equation involving the "acceleration"  $\ddot{z}$  is analogous to Newton's equation of motion. The answer provides insight into the behavior of rays in deep sound channels and bears directly on the raytracing routine employed in RAY1 and RAY2. The Euler-Lagrange equation, which follows as a theorem<sup>3</sup> from the variational principle in eq (2), as mentioned above, states that

$$(d/dt) \partial L/\partial \dot{q} - \partial L/\partial q = 0 \quad (6)$$

If the reader applies the transformation given in eq (5) then, after some algebraic manipulation, eq (6) will be seen to become

$$\ddot{z} = -(1 + \dot{z}^2) c^{-1} \partial c/\partial z + \dot{z}(1 + \dot{z}^2) c^{-1} \partial c/\partial x \quad (7)$$

a result obtained previously by Milder.<sup>2,4</sup> Equation (7) is similar to Newton's equation of motion, giving the acceleration as a function of displacement, velocity, and time.

RAY1 and RAY2 use a fourth order Runge-Kutta scheme<sup>2</sup> to integrate eq (7), and thus obtain the ray depth as a function of range. Equation (7) describes the ray

4. Milder DM, *Ray and Wave Invariants for SOFAR Channel Propagation*, J. Acoust. Soc. Am., v. 46, p. 1259-1263 (1969).

curvature in terms of the local sound speed derivatives in depth and range and the ray slope. For prescribed initial conditions  $z(0)$  and  $\dot{z}(0)$ , and a given function  $c(z; x)$ , it specifies a unique trajectory satisfying Fermat's principle.

When the medium is range-independent, the second term on the right-hand side of eq (7) vanishes. A further simplification comes about since in range-independent media Snell's law holds in the form  $c_v = c/\cos\theta$ , where  $c_v$  is the constant vertexing speed (where  $\dot{z} = 0$ ). Thus eq (7) becomes

$$\ddot{z} = -c_v^2 (dc/dz) c^{-3} = -(\partial/\partial z) (-c_v^2/2c^2) \quad (8)$$

Hence in range-independent SVPs the motion of a ray is precisely analogous to the trajectory of a mechanical particle of unit mass under the action of a potential field given by

$$V(z) = -c_v^2/2c^2 \quad (9)$$

This result allows considerable insight into the trajectories of rays. For example, if we consider the Hirsch profile

$$c(z) = c_0/(1 - z^2/a^2)^{1/2}$$

then the potential is

$$\begin{aligned} V(z) &= -(c_v/c_0)^2 (1 - z^2/a^2) \\ &= (c_v/c_0 a)^2 z^2 + \text{const} \end{aligned}$$

which is a quadratic function of  $z$ , the same as a simple harmonic oscillator. Ray paths must therefore be sine waves in this SVP. It is simple to sketch potential functions for any reasonable SVP, and range-dependence may be included in this analogy by allowing  $V(z)$  to vary slowly with time.

When the medium is range-dependent, then the analogous classical mechanics problem involves a time-dependent potential, as one can see from the transformation eq (5). Hence the energy of the analogous particle is not conserved, nor are the positions of the turning points where  $\dot{q} = 0$  or  $\dot{z} = 0$ . If the variations are gradual, however, the action integral

$$J = \oint p dq \quad (10)$$

is approximately conserved.<sup>3</sup> Here  $p \equiv \partial L/\partial \dot{q}$ ;  $p$  is called the momentum canonically conjugate to the coordinate  $q$  in classical mechanics. If the reader again applies eq (5) and uses  $\dot{z} = \tan\theta$ , he will find

$$p = \dot{z}/c (1 + \dot{z}^2)^{1/2} = \sin\theta/c$$

and thus eq (1) follows as the adiabatic invariant for sound rays. Note that the integral covers one cycle of the trajectory and represents the area of an (almost) closed loop traced

out in p-q space, known as phase space. The path is a closed loop for range-independent SVPs.

## 2. AIA Algorithm for Average Horizontal Ray Velocity

One may use the invariance of  $J$  to compute the average horizontal velocity of a ray traversing a range-dependent SVP as follows. We assume it is possible to break up the entire region of interest into local regions bounded by some set of contiguous contours inside each of which  $c(z)$  is a known function, which can be regarded as range-independent within the local region.

First one constructs tables showing the relationship between  $J$  and  $\bar{c}$ , the average horizontal ray velocity, for each local region. This may require tracing perhaps 10 to 50 rays for each SVP. Each ray need only be traced for a small number of cycles (one or two) to find  $J$  and  $\bar{c}$  for the given initial conditions. These tables then allow one to find how  $\bar{c}$  varies from region to region for a particular  $J$  value, by employing simple table-look-up procedures.

This method does not yield detailed information on the trajectory, such as positions of ray turning points in range, but this is the cost of obtaining estimates of  $\bar{c}$  for long-range paths with simple algorithms. For a prescribed path, one then may find the effective signal speed for given initial conditions (depth and ray angle) from the  $\bar{c}$  values in each region according to the fraction of time spent in each region. If  $R$  denotes the total range,  $R_i$  the distance traveled in region  $i$ , and  $\bar{c}_i$  the average horizontal velocity in region  $i$ , then the effective signal speed is given by

$$\bar{c} = R / \sum_i (R_i / \bar{c}_i) \quad (11)$$

Additional algorithms are necessary to select a range of initial conditions that characterize rays which carry most of the acoustic energy. Depending on the geometry, these may range from simple inspection procedures to complicated ray-trace routines requiring detailed bathymetry charts. Reference 2 discusses possible methods for selecting appropriate ranges of  $J$  values using the output of RAY2 (see section VI). Further remarks on this are included in section IIC, where we indicate how certain of the quantities computed by RAY2 facilitate ray selection.

## B. GENERAL DESCRIPTION OF RAY1

A listing of the code RAY1 will be found in section V, and instructions on its use in section III. Here we shall describe the general features of RAY1.

RAY1 provides quantitative answers to the question of the validity of the AIA. Earlier we noted that  $J$  is conserved for sufficiently slow variations in the SVP. More precisely,  $J$  is conserved (or nearly so) provided that any changes in the SVP are fractionally small over one cycle distance (in range) of the ray. This follows from the fundamental law of ray theory, Fermat's principle of least time<sup>3</sup> as discussed in section II.A.1. We refer the reader desiring further discussion of this to Landau and Lifshitz<sup>3</sup> and the bibliography of reference 2.

In real ocean environments, the adiabatic condition is satisfied for RR (Refracted Refracted) rays, but one still may ask what degree of inhomogeneity is required before the AIA fails badly. RAY1 provides specific answers to this by allowing the user to control the horizontal gradients of parameters in the SVP function. Thus both the degree of inhomogeneity and the effect of the functional form  $c(z)$  may be investigated.

Presently three self-similar SVPs are available as subroutines in RAY1. They are the parabolic profile,

$$c(z, x) = c_0(z) [1 + z^2/a^2(x)] \quad , \quad (12a)$$

the Hirsch profile,

$$c(z, x) = c_0(z) [1 - z^2/a^2(x)]^{-1/2} \quad , \quad (12b)$$

and the bilinear profile,

$$c(z, x) = c_0(x) [1 \pm z/a(x)] \quad , \quad z > 0 (< 0) \quad (12c)$$

Figure 1 shows these SVPs for range-independent SVPs. Each of equations (3) describes a slab symmetric (depending only on range  $x$  and depth  $z$ ) sound channel with an axis at  $z = 0$ , and an axial sound speed  $c_0(x)$ . Both  $c_0(x)$  and  $a(x)$  are linear functions of  $x$  in the current version of RAY1. By varying their derivatives with appropriate input data, the user may study the degree to which nonadiabatic changes in the SVP affect the action integral, or the discrepancy between the computed average horizontal ray velocity and the predicted value, assuming  $\partial J/\partial x = 0$ . Details on the program inputs will be deferred until section III.

RAY1 allows the user to select one of the three SVPs, and control tracing of rays in the presence of constricting (if  $da/dx < 0$ ) or widening ( $da/dx > 0$ ) sound channels. Gradients in  $c_0$  and  $a$  are independent. In addition, the raytracing routine employed (a fourth order Runge-Kutta algorithm applied to the Euler-Lagrange equation of motion obtained from Fermat's principle) has an automatic test and redefinition routine which refines the step size  $dx$  when there are fewer than 150 steps per half-cycle, although this number can be easily modified (see section V).

For completeness, we present in table 1 the analytic formulae for ray paths and the average horizontal ray velocity in each of the SVPs in RAY1 for range-independent conditions. For the parabolic SVP,  $u_1$  and  $E(u_1)$  are the normal elliptic integrals of the first and second kind, respectively, with argument  $z/a$ , modulus squared  $(\alpha-1)^2/2(\alpha^2+1)$  where  $\alpha^2 \equiv c_v/c_0$ ;  $sn u_1$ ,  $cn u_1$  and  $dn u_1$  are Jacobian elliptic functions;  $E(k)$ ,  $K(k)$  and  $\Pi(\beta^2, k)$  are complete elliptic integrals of the first, second, and third kind with  $k^2 = (\alpha-1)^2/(2\alpha^2+2)$  and the parameter  $\beta^2 = (1-\cos\theta_0)/2$ .<sup>5</sup>  $\theta_0$  is the angle with respect to horizontal at which the ray crosses the sound channel axis at  $z = 0$  in all formulae.

Figures 2 and 3 show the agreement found for  $\theta_0(0) = 30^\circ$  in an earlier study<sup>2</sup> between predicted sound speeds, assuming  $\partial J/\partial x = 0$ , and those computed by RAY1 in the

5. Byrd, PF and Friedman, MD, *Handbook of Elliptic Integrals for Engineers and Scientists*, Springer Verlag, New York (1971).

presence of various gradients in  $a(x)$ , the depth scaling function. The agreement generally is good even when the environment changes rapidly, for example by 40% (in  $a(x)$ ) in a single ray cycle. Such agreement, although it cannot be expected for all SVP choices, lends considerable support to the general validity of the AIA. Quantitative answers to this question are of interest since the AIA method seems to offer a simple solution to some time difference fixing (TDF) problems: data bases for implementing AIA sound speed algorithms are easily generated, the table-look-up AIA computations typically are far less time-consuming than long-range raytracing, and the method permits very flexible updating of data in individual SVP regions without requiring long-range raytracing computations to be repeated.

In figures 2 and 3  $x_p$  is the cycle distance and  $x_c$  the critical range at which the channel constricts to an extent such that rays are reflected, and cannot propagate further. The notation  $x_c/x_p (x=0)$  is the ratio of the critical range to a cycle distance, evaluated at the initial range. Thus, for example, if  $x_c/x_p = 3$ , the critical constriction occurs only 3 cycle distances from the ray's starting point. The vertical axis is the normalized average horizontal ray speed ( $\bar{c}^* = 1$  for a ray on the channel axis) and the horizontal axis is the normalized channel width parameter ( $a^* = a/a_0$  where  $a$  is the scale length in the table 1 formulas, and  $a_0$  is the initial value of  $a$ ).

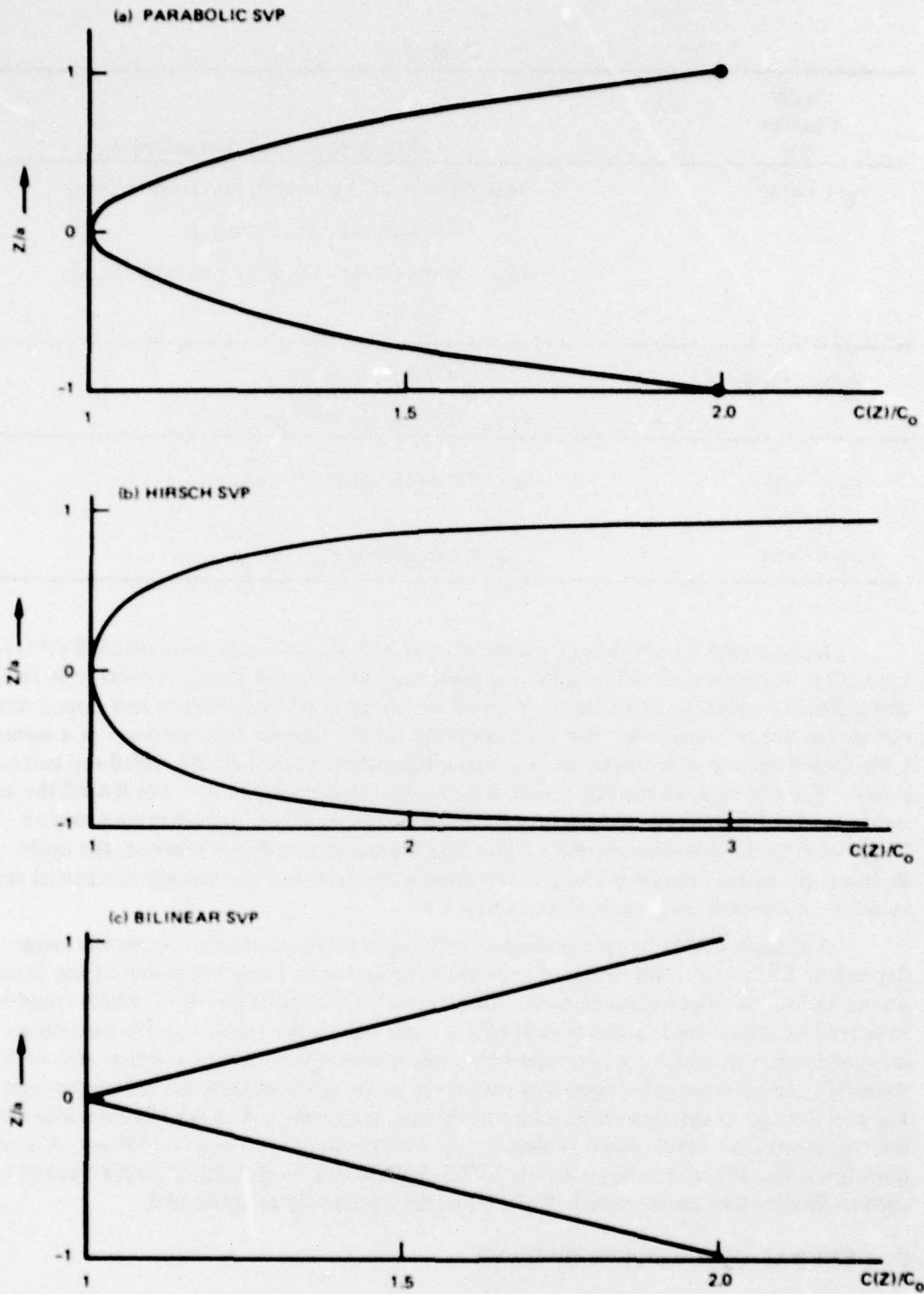


Figure 1. Three analytical forms for model sound velocity profiles (from eq (12)) in dimensionless form.

Table 1.

SVP Function $c(z)$	Ray Trajectory and Average Speed
$c_0(1 + z^2/a^2)$	$x/a = (2\alpha^2 + 2)^{-1/2} [(2\alpha^2 + 2) E(u_1) - (\alpha^2 + 2\alpha)u_1$ $- (\alpha - 1)^2 \operatorname{sn} u_1 \operatorname{cn} u_1 / \operatorname{dn} u_1]$ $\bar{c}/c_0 = \sec\theta_0 (2E(k) - K(k)) / [(1 + \sec\theta_0) \Pi(\beta^2, k) - K(k)]$
$c_0(1 - z^2/a^2)^{-1/2}$	$z = a \sin\theta_0 \cos(x/a \cos\theta_0)$ $\bar{c}/c_0 = 2 \cos\theta_0 / (1 + \cos^2\theta_0)$
$c_0(1 \mp z/a)$	$(z/a + 1)^2 + (x/a - \tan\theta_0)^2 = \sec^2\theta_0$
$z < 0 (> 0)$	$\bar{c}/c_0 = \tan\theta_0 / \operatorname{kn}(\sec\theta_0 + \tan\theta_0)$

Input to RAY1 consists of a control or switch variable indicating which SVP is to be used, a set of parameters defining the medium (e.g., axial sound speed, vertical scale factor, and gradients with respect to range), a set of initial ray conditions (depth and slope), and parameters for the range step size and maximum range. Output is in the form of a summary table listing the ray coordinates at each vertexing point. These are also called ray turning points. For RR rays, all turning points are characterized by  $dz/dx = 0$ . (In RAY2 the surface reflection for RSR (Refracted-Surface-Reflected) rays leads to a discontinuous slope.) In addition to the coordinates, RAY1 also lists the maximum depth reached, the cycle distance, the phase integral evaluated over each half-cycle, and the average horizontal ray velocity. Examples are presented in section VI.

Although RAY1 has established that the AIA works well even in severely range-dependent SVPs of certain kinds, one should note that only linear variations of the depth scaling factor have been programmed. An extremely interesting question, which could be answered by minor modifications in RAY1, involves the conservation of  $J$  in two range-independent SVPs which are connected by some inhomogeneous region where  $a(x)$  varies smoothly. In each range-independent region the phase space trajectories are closed, and  $J$  is well defined as the area enclosed by the phase space orbit. As RAY1 is currently written, the trajectories are never closed (unless the user inputs  $da/dx = 0$  as a condition). A second question is the effect of nonsymmetric SVPs. With minor modifications, RAY1 could be used to study other more realistic SVPs than those presently programmed.

### C. GENERAL DESCRIPTION OF RAY2

RAY2 consists of four Fortran routines which trace a family of rays in a user supplied SVP, computing for each ray the turning point coordinates (depth, range, and time), the

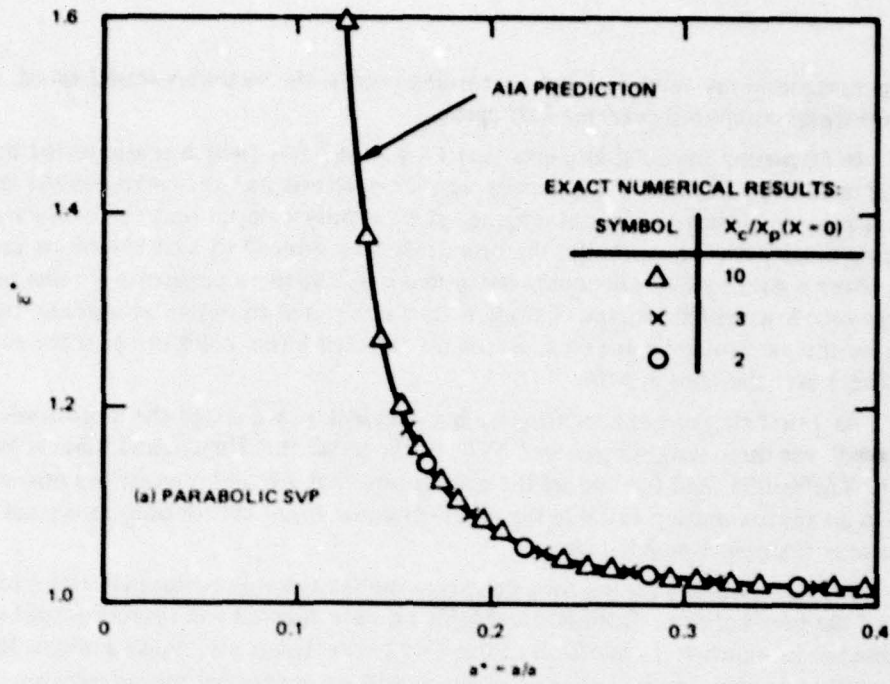


Figure 2. Comparison of AIA predictions and exact numerical results for parabolic SVP (from ref. 2).

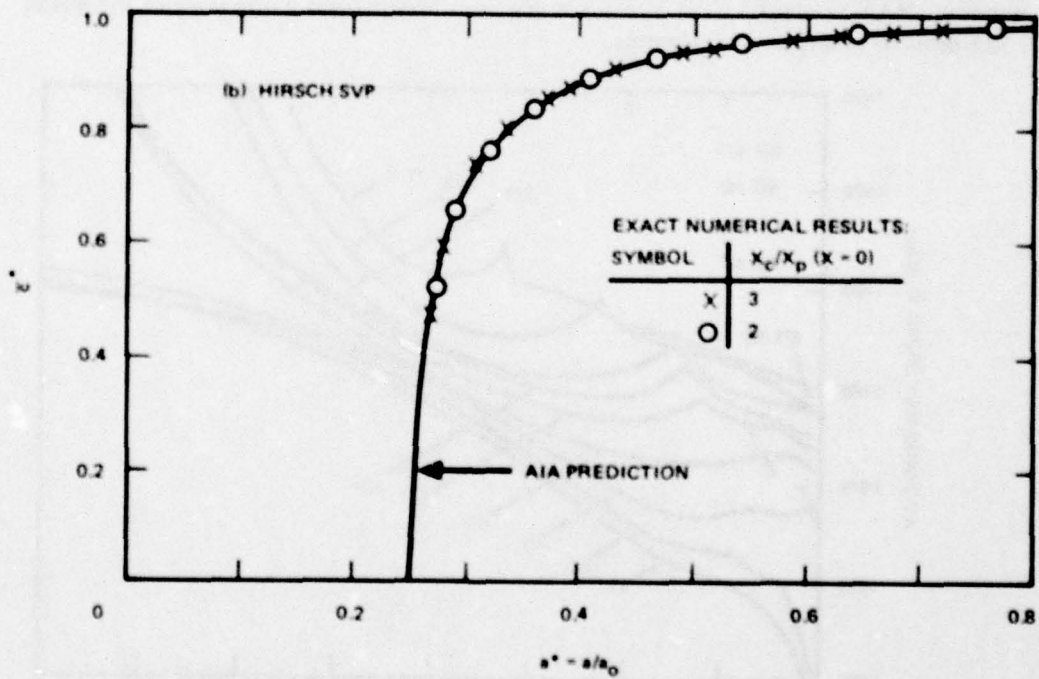


Figure 3. Comparison of AIA predictions and exact numerical results for a Hirsch SVP (from ref. 2).

average horizontal ray velocity between turning points, the vertexing sound speed, and the action integral computed over one-half cycle.

In discussing the adiabatic invariant  $J = \oint (\sin\theta) dz/c$  (which is also called the action integral in analogy to classical mechanics, or the phase integral since it represents an area in phase space) we outlined a general scheme for efficiently computing an effective signal speed over long-range paths. Essentially, the procedure was reduced to a table-look-up method to obtain from a data base of previously computed  $\bar{c}$  vs  $J$  tables a particular  $\bar{c}$  value in each SVP region. A weighted average of these is then computed to obtain an average sound speed for the particular  $J$  value (that is, for the selected initial conditions for the ray trajectory) over the chosen path.

As a first step in implementing such an algorithm, we tested the hypothesis "J is conserved" for three range-dependent SVPs of the parabolic, Hirsch, and bilinear types using RAY1. The results tend to support the assumption that J is an invariant in range-dependent SVPs to an approximation suitable for practical signal speed calculations in typical ocean environments supporting RR rays.<sup>2</sup>

RAY2 provides a means for calculating the relationship between  $\bar{c}$  and J for arbitrary SVPs of the user's choice. Both RR and RSR rays are allowed and typical output can be presented as in figure 4. In addition to the  $\bar{c}$  vs J curves, one also needs a means for selecting an interval of J values characterizing the rays which carry most of the acoustic signal energy. This may be done by eliminating rays which exceed a cut-off depth or by including only those rays launched from the source (or arriving at the receiver) within a fixed angular window. RAY2 provides a list of ray turning point depths and a summary of the initial conditions to facilitate this selection.

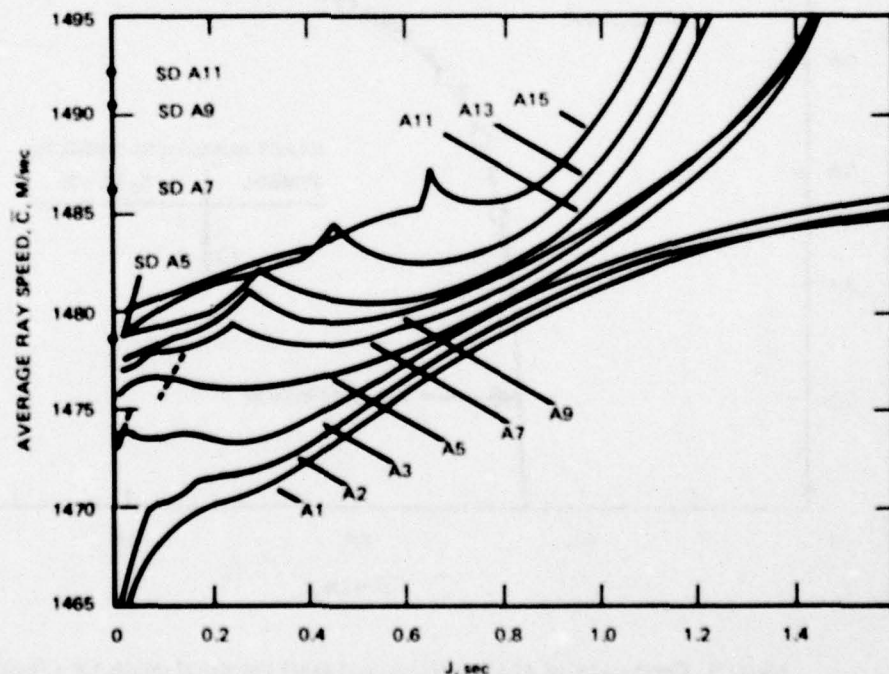


Figure 4. Relation between  $\bar{c}$  and J for a selection of SVPs (ref. 2).

Further discussion of RAY2, including input data requirements and internal logic, will be found in sections IV and V. It is worthwhile to stress here that RAY2 treats rays only in homogeneous (range independent) SVPs, and traces a family of 40 rays covering  $0.5^\circ$  to  $20^\circ$  in depression angle at the source out to the fifth vertexing point. (The latter parameters are simply adjusted by internal code changes.) Rays are traced over several half-cycles, even though a single half-cycle suffices to find  $\bar{c}$  and J, in order to check the accumulation of round-off errors in the integration routine. Since one is free to refine the mesh size, the trajectory may be made to reproduce itself on each loop to any accuracy (subject to machine constraints). One should use as large a step size as is compatible with the accuracy desired in order to minimize computations.

### III. INSTRUCTIONS FOR USING RAY1

Here we describe the required input data, output format, and general interpretation of results for RAY1.

#### A. INPUT REQUIREMENTS

Input data is read from cards under the Fortran free-field format. This format specification requires commas between separate data items but allows the items to be positioned arbitrarily on a data card. If a single read statement causes the input of data continued on to subsequent cards, no comma is required after the last item on each card. In this case, the card end itself serves as a legal delimiter between successive items.

On the first card, the integer variable ICASE must be punched. This should be the number of rays to be traced.

On the second card, and the remaining ICASE-1 cards, the data items as shown in table 2 must be punched. Typically one card is adequate to enter all items for a ray.

#### B. OUTPUT

RAY1 allows a quick check of the input data, by printing the variables for each case (each ray) considered in the form

```
CASE 1
DX = 1.2-02 METERS
XMAX = 1.180000+01 M
GRAD 1 = - 6.3510-02 (CHANNEL WIDTH GRADIENT)
GRAD 2 = 0.0000 Hz (AXIAL SPEED GRADIENT IN RANGE)
CO = 1.0000+00 M/SEC
AO = 1.0000+00 M
ZDOT = 3.6397 - 01 RADIANS or 2.0000+01 DEGREES
ZO = 0.0000 M
PROFILE: 1 (1=HIRSCH, 2=PARABOLIC, 3=BILINEAR)
```

If the mesh was refined during any cycle, the next line(s) will present this information in the form

```
MESH = 2 AT STEP 814
```

Table 2.

Card	Fortran Variable Name	Definition in RAY1
1	ICASE	Number of rays to be traced
2	DX	Range increment for Runge-Kutta raytracing routine (meters)
	XMAX	Cut-off range for raytracing (meters)
	GRAD1	Gradient in vertical scale length $a(x)$
	GRAD2	Gradient in axial sound speed $c_0(x)$ (Hz)
	CO	Initial axial sound speed (m/sec)
	AO	Initial vertical scale factor (meters)
	ZDOT	Initial ray slope ( $\tan\theta_0$ )
	ZO	Initial ray depth (meters)
	IPRINT	Control variable for printing a detailed path (0 : no ; 1 : yes)
	ITYPE	Control variable for SVP type (1 : Hirsch ; 2 : parabolic ; 3 : bilinear)
3	DX,....,ITYPE	Data for next ray

indicating one-half the input step size was used past step 814. These lines will not appear if no step size adjustment was made.

RAY1 employs a cut-off not only in range, but also in the number of steps calculated (presently 9999 steps are done) and in the channel width parameter. The user may inadvertently set up a constricting sound channel such that  $a(x)$  becomes zero and then negative in the allowed range. Raytracing is meaningless for such a profile. Rather than "bombing" under such conditions, RAY1 will test  $a(x)$ , find it is nonpositive, print a message of the form

CHANNEL WIDTH LESS THAN 0.01 AT STEP 704

terminate raytracing of the present ray, and go on to the next case, if there is one.

After RAY1 has completed tracing a given ray to XMAX (or for 9999 steps, or until  $a(x) \leq 0$ , whichever occurs first), it prints the summary, beginning with the number of axis crossings. (In contrast to RAY2 where the ocean surface is at  $z = 0$ , RAY1 always sets  $z = 0$  at the channel axis.) Then, for each axis crossing, the following data are printed:

STEP	RANGE	TIME	AVG(DX/DT)	A/AO	MAX Z	XP/AO	J
NO	(M)	(SEC)	(M/SEC)		(M)		(SEC)

Here AO denotes the initial value of the channel width parameter, and A/AO the dimensionless local value of  $a(x)$ . This is the same function  $a(x)$  appearing in eq (12) above. For constricting channels, the numbers in the A/AO column should be monotonically decreasing.

It is worthwhile noting that the AVG(DX/DT) column is derived from pairs of axis crossings and the first value corresponds to the average range rate or horizontal velocity between the initial ray position and the first turning point. For this reason, it may not represent an average between turning points. For the same reason, the last value is arbitrarily set to zero, there being no point beyond the last turning point with which to calculate  $\bar{c}$ . Similar comments apply to the entries in the J column, the (dimensionless) cycle period column XP/AO, and the maximum depth column.

#### IV. INSTRUCTIONS FOR USING RAY2

In this section we present information required to understand and run RAY2, beginning with a brief description of the necessary input parameters and the appropriate format for these, the output, and details of the program's scope and internal logical structure.

##### A. INPUT PARAMETER LIST

RAY2 consists of routines for tracing rays in user-provided SVPs. A cubic spline<sup>6</sup> is used to smooth the input data and to calculate interpolated values and derivatives of  $c(z)$  required by the Runge-Kutta routine. Output is provided in a summary form similar to that of RAY1. Detailed instructions for using RAY2 are provided in section IV, and section V contains a listing on the Fortran source code. All input data must be read from cards. Since freefield format is used for input (with one exception, an alphanumeric header card) one may simply place data items, in sequence, in any fields on the cards. Commas must appear between successive items, except when the next card is a continuation of the same read list items. This often occurs for the SVP data. In this case, the end of the card itself acts as a legal delimiter between the last item on the given card and the first item on the next card, and no comma is required.

RAY2 requires the input shown in table 3 immediately after the usual @XQT RAY2.ABS statement.

The variable NOSVPS tells RAY2 how many SVP functions are to follow. If this card is incorrectly punched (or misread), RAY2 will either end its computations before reaching the last data set or attempt to read beyond the last data set provided. If this card is missing, RAY2 will recognize NPTS as NOSVPS, and then fail (probably with a fatal execution error) when attempting to read card 3 under the format 2I10,2A6.

On card 2, NPTS is the number of pairs of depth (ZSVP) and sound speed (CSVP) values comprising the first SVP. If NPTS is mispunched RAY2 may attempt to read past the last card, or may stop before reading the last card, and proceed to recognize card j+1 as SVP data or SVP data as card j+1. Results of such input errors could include many forms of abnormal termination.

Immediately following NPTS is IUNITS, which indicates the choice of units made by the user for SVP data. Set IUNITS equal to 1 if the units are to be meters and meters per second and 2 if feet and feet per second.

6. Mathpac, Univac Corp. (SPLN1 and SPLN2 are documented in a number of manuals covering resident subroutines.)

Table 3.

Card Number	Fortran Variable or Array Name	Input Format Spec (Variable Type)
1	NOSVPS	Free Field (Integer)
2	NPTS, IUNITS, MSG(1) MSG(2)	2110,2A6
3	ZSVP(1), CSVP(1) ... ZSVP(i), CSVP(i)	Free Field (Real)
4	ZSVP(i+1), CSVP(i+1),	Free Field (Real)
...	...	
j	... ZSVP(NPTS), CSVP(NPTS)	Free Field (Real)
j+1	DX, ZO, ZMAX, IPLOT	Free Field (Real, Real, Real, Integer)
j+2,	data for next SVP, beginning with NPTS.	
...	IUNITS, MSG(1),	
...	MSG(2), and ending	
k	with DX, ZO, etc.	
k+1,	data for last of	
etc.	NOSVPS data sets	

MSG(1) and MSG(2) provide a title for the SVP to follow, consisting of 12 characters selected from the full range of UNIVAC 1110 Fortran and entered in columns 21-32 of card 2.

Note that card 2 is read under a formatted input specification.

Beginning with card 3, and continuing on subsequent cards if necessary, is the first set of SVP data. As many pairs may be entered on one card as space permits and pairs of (ZSVP, CSVP) values may be split, with ZSVP(i) ending one card and CSVP(i) beginning the next card.

Four variables which control raytracing are entered on the card after the last SVP data card. DX, ZO, and ZMAX are the range increment for the Runge-Kutta algorithm, the initial ray depth, and the maximum depth allowed for a ray, respectively. *These variables are interpreted by RAY2 as being expressed in meters.* IPLOT should be set to 0 if one desires printed output, and 1 if plots are desired in addition. Typical values for DX should be approximately one-sixteenth of a ray cycle period, for coarse results, and less for more accurate raytracing. If a ray exceeds depth ZMAX, the remaining (steeper) rays are not traced and RAY2 attempts to read the next SVP data set.

## B. OUTPUT

RAY2 is designed to allow the user an immediate check of all input. The first line printed after the @XQT statement should agree with the input variable NOSVPS, and reads:

\*\*\* THIS RUN CONSISTS OF (NOSVPS) SVP(S) \*\*\*

The second output line consists of the 12 character message string MSG(1), MSG(2) imbedded as follows:

\*\*\* SVP : (MSG(1), MSG(2)) \*\*\*

This simply identifies the particular SVP being computed. If several SVPs are to be run, one such header message appears at the start of the output for each SVP.

The header message is followed immediately by a line that checks the choice of units for the SVP data, and reads:

USER INPUT UNITS FOR THE SVP : (1 or 2) (1 : M, M/SEC ; 2 : FT, FT/SEC)

IUNITS and the units choice (1 or 2) should agree. Next the SVP is printed as a pair of columns labeled DEPTH and c. There should be NPTS pairs of values.

After the SVP data, RAY2 prints the control parameters specifying how rays are to be traced, namely DX, ZO, and ZMAX.

Beginning with the line

CASE NUMBER : 1 .

RAY2 prints, as presently structured, 40 ray-path summaries, for the rays which are launched from depth ZO at the angles  $-0.5^\circ$ ,  $-1.0^\circ$ ,  $-1.5^\circ$ , ...,  $-20^\circ$ , with respect to horizontal. Each case is summarized by a set of initial conditions printed in the form

CASE NUMBER : 1  
INITIAL ANGLE = 0.5 DEGREES  
INITIAL SOUND SPEED = 1495.6 M/SEC  
PREDICTED VERTEXING SPEED = 1500.2 M/SEC

The first and second lines are redundant since the initial angle associated with a given case is always one-half the case number. Nevertheless, it is useful to see at a glance the angle of the ray being considered, and if internal changes are made to produce a different angular interval for rays, these two lines would serve as checks on the code changes and would simplify some data analysis.

The initial sound speed is computed by the spline curve fitting routine SPLN1,<sup>6</sup> and used to compute a predicted vertex speed according to Snell's law,

$$c_{\text{vertex}} = c(z_0) / \cos\theta(z_0) .$$

Each case is also summarized by a table showing the history of ray turning points. As presently written RAY2 automatically traces rays through four turning points. The variables printed at each turning point (with the exception of J for the first turning point and the average speed for the last turning point) are:

K, XTP, TTP, ZTP, CTP, J(K), AVGSP .

These stand for the turning point number,  $K$ , the range to the  $K$ th turning point, the time elapsed at the  $K$ th turning point, the depth of the  $K$ th turning point, the ray speed at the  $K$ th turning point, the action integral  $\int \sin\theta dz/c$  computed over the last one-half cycle, and the average horizontal ray speed from the  $K$ th to the  $(K+1)$ st turning point.

Figure 5 illustrates the physical significance of these summary data items. Note that the first value printed in the  $J$  column is really an incomplete integral, evaluated from the starting depth  $z_0$  to the first turning point, and should be ignored. RAY2 computes the average horizontal ray velocity between pairs of turning points. The first AVGSP value printed out is associated with the first and second turning points, and the fourth value is automatically set to zero.

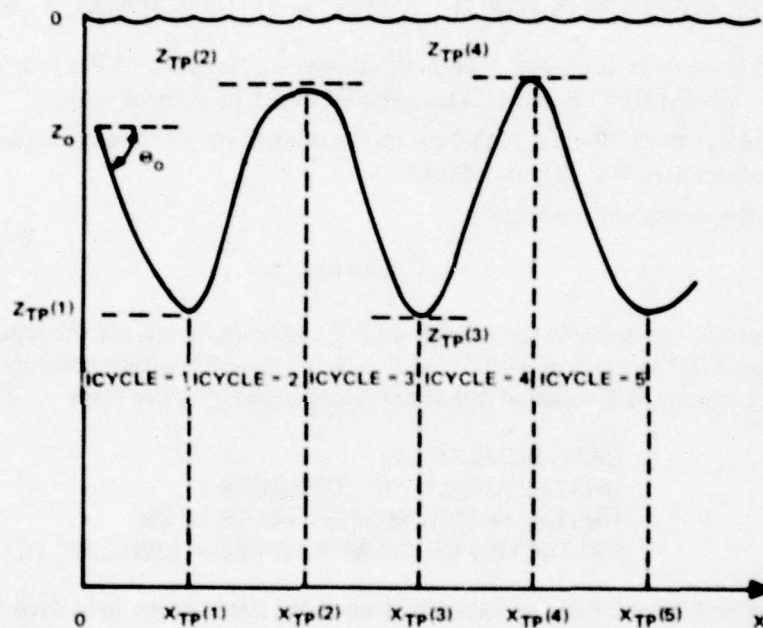


Figure 5. A sketch of the physical meaning of the summary data items in RAY2.

## V. INTERNAL LOGICAL STRUCTURE OF RAY1 AND RAY2

In this section we shall describe the logical structure of the Fortran routines comprising RAY1 and RAY2. Special emphasis is placed on the areas in which slight modifications in these codes would enhance their usefulness, particularly in the direction of permitting better output (e.g., plots) and more flexibility through user-selected input variables beyond those now available.

### A. INTERNAL STRUCTURE OF RAY1

As it is presently written, RAY1 contains comment cards defining most of the variables of interest (see section VI). A flowchart of RAY1 appears in figure 6. ICASE is

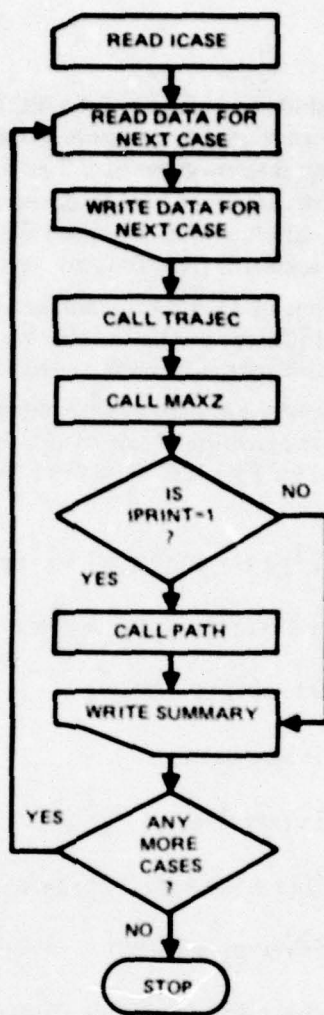


Figure 6. Flowchart of RAY1.

the number of cases to be considered. Each case consists of a particular choice for an SVP, initial ray depth and slope, and parameters for the range step, maximum range, and gradients of the range-dependent parameters (axial sound speed and channel width parameter in eq (12)). In addition, RAY1 reads IPRINT which allows or suppresses a longer printout of the trajectory.

An extremely valuable addition to RAY1 would be a plotting routine which simply plots the ray paths. One could then observe immediately (without calling the subroutine PATH) the effect of squeezing or expanding SVPs on ray paths. A second much needed improvement consists of permitting several rays to be traced in a given range-dependent SVP, without the requirement of punching all SVP data and other parameters anew for each ray.

The subroutine TRAJEC computes a ray path, including the time and average horizontal velocity at each turning point, and the action integral over each half-cycle. Beginning at line 26 (see section VI) TRAJEC computes the new ray slope (DERIZ). These instructions end at line 40 of TRAJEC, and consist of the Runge-Kutta algorithm mentioned earlier.

Once an advanced value of  $z$  is found, TRAJEC finds the new sound speed at this depth and range, which in turn is used to compute a time increment given by  $\Delta t = \Delta s/c$ , and a new increment of the action integral given by  $c^{-1} \sin\theta \Delta z$ . These steps correspond to lines 42 through 55. Two tests are made here to insure that the user has not allowed the channel width parameter to vanish, and to avoid any illegal (or rather invalid) reference to array elements by looking backwards from the very first step of the raytracing.

The remaining portions of TRAJEC handle axis crossings and adjust the step size should there be fewer than 150 steps per half-cycle. We recommend that an input variable be added to permit varying this particular choice at run time.

In section II we derived the Euler-Lagrange equation, eq (7), for Fermat's variational principle. RAY1 calculates the right-hand side of this equation of motion in the function subroutine F, which is called by TRAJEC. The three SVPs in equations (12) lead, respectively, to the results

$$F = -2(1 + \dot{z}^2) z/(a^2 + z^2) + \dot{z}(1 + \dot{z}^2) g_2/c_0 - 2 \dot{z}(1 + \dot{z}^2) (z^2/a) g_1/(a^2 + z^2) , \quad (13a)$$

$$F = -(z/a)^2 (1 + \dot{z}^2)/(1 - (z/a)^2) + \dot{z}(1 + \dot{z}^2) g_2/c_0 - \dot{z}(1 + \dot{z}^2) (z^2/a^3) g_1/(1 - z^2/a^2) , \quad (13b)$$

$$F = \pm(1 + \dot{z}^2)/(a + |z|) + \dot{z}(1 + \dot{z}^2) g_2/c_0 - \dot{z}(1 + \dot{z}^2) |z| g_1/a(a + |z|) , \quad z < 0 (> 0) , \quad (13c)$$

as one can verify easily by direct differentiation. Here  $g_1$  and  $g_2$  are respectively  $da/dx$  and  $dc(z=0)/dx$ .

MAXZ and PATH are short routines. The former searches each half cycle of the trajectory and returns a list of the maximum off-axis distance reached by the ray. The latter prints 250 points equally spaced along the trajectory, or as many points as are found before the maximum range is reached.

RAY1 should be expanded to handle a wider class of range-dependent analytic SVPs, and to permit connecting range-independent SVPs smoothly, as discussed in section II.

## B. INTERNAL STRUCTURE OF RAY2

RAY2 consists of only two routines and two cubic spline routines resident on the NOSC UNIVAC 1110.<sup>6</sup> Unlike RAY1, RAY2 does provide a plot subroutine and uses any user-provided SVP. We recommend that the plot routine calls be modified to allow several rays to be plotted on a single graph. Also desirable would be a plot of the user-input SVP as smoothed by the spline routines.

A flowchart of RAY2 is given in figure 7. Although somewhat complicated in appearance, the flowchart involves only three basic loops. The outermost, which corresponds

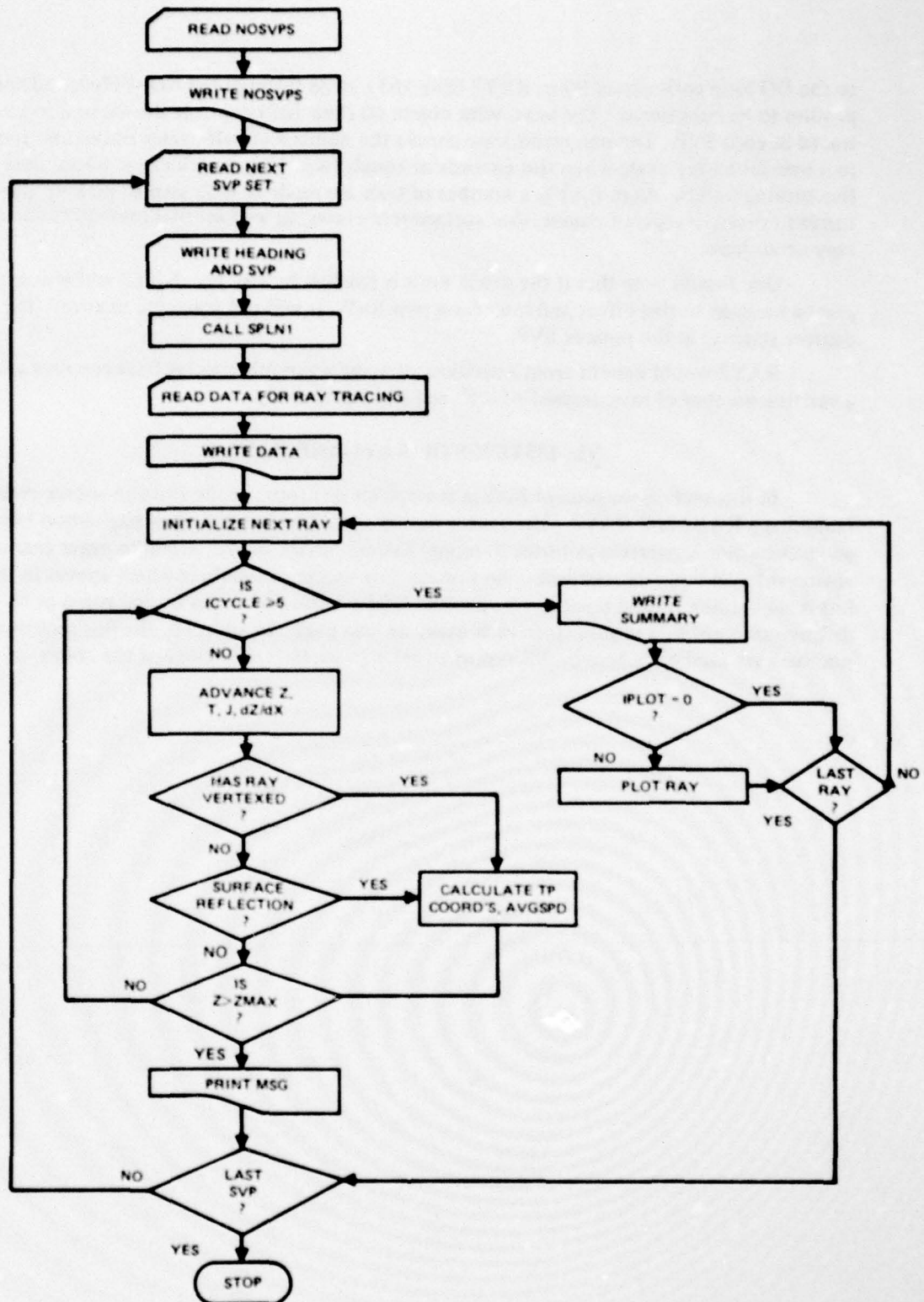


Figure 7. Flowchart of RAY2.

to the DO loop with object 90 in RAY2 (line 163), steps through the NOSVPS sound speed profiles to be considered. The next, with object 60 (line 162) controls the 40 rays to be traced in each SVP. The innermost loop checks the number of half-cycles traced and jumps to a new initial ray angle when this exceeds or equals five. Hence each ray is traced over five turning points. As in RAY1, a number of tests are made at each step to pick up the turning points, except, of course, that surface reflections, as well as total internal reflections, may occur here.

One should note that if the depth limit is reached by any ray, RAY2 will automatically print a message to this effect and look for a new SVP. It will not trace the next ray (0.5 degrees steeper) in the present SVP.

RAY2 would benefit from a revision allowing a variable spacing between rays and a variable number of rays, instead of  $0.5^\circ$  and 40, respectively.

## VI. LISTINGS OF RAY1 AND RAY2

In this section we present listings (computer printout) of the Fortran source code comprising RAY1 and RAY2. The reader should note that in some cases pagination becomes awkward when converting printout to report format. In particular, separate pages cannot always refer to separate routines. The Fortran line sequence numbers which appear in the left-hand column should therefore be used to follow a routine across several pages or to distinguish multiple routines from each other on one page. In addition, the line sequence numbers are used elsewhere in this report to refer to particular sections of the codes.









00003 MAY.PATH  
FOR SHE3-02/15/70-11:00:01 (17.)

SUBROUTINE PATH ENTRY POINT 000006

STORAGE USED: CORE(1) 00007Z; DATA(0) 00007; BLANK COMMON(1) 000000

COMMON BLOCKS:

0003 DATA 000011  
0004 RESULT 170077

EXTERNAL REFERENCES (BLOCK, NAME)

0005 MNDUS  
0006 M1026  
0007 MEND30

```
00101 SUBROUTINE PATH  
00103 COMMON/DATA/02,UMAX,GMAD1,GMAD2,CO,AD,2001,20,TYPE  
00104 COMMON/RESULT/2,100001,1100001,11100001,11100001,0EM12,100001,ICOUNT,  
00105 * J12001,AV12001,2*AV12001,ACT10N12001,AV12001,T012001,AV12001,N  
00106 WRITE(6,101)  
00107 101 FORMAT(10, ' MAY TRAJECTORY: '// STEP NO. 'PANG',  
00108 * 05, 'DEPTH', 58, 'CHANNEL', 48, 'TIME',  
00109 * 128, 'IM1', 78, 'IM1', 78, 'MIDTIME', 48, '(SEC)')  
00110 GO TO 101,N  
00111 ATMP=AO*GMAD1*0.1111  
00112 P=0.1111  
00113 IF 10.66,UMAX, RETURN  
00114 10 IF MOD(1,61.63,0) WRITE(6,102),P,2(11),ATMP,TYPE  
00115 102 FORMAT(16,48,41P(10,41))  
00116 RETURN  
00117 END  
00002  
00003  
00004  
00005  
00006  
00007  
00008  
00009  
00010  
00011  
00012  
00013  
00014  
00015  
00016  
00017  
00018  
00019  
00020  
00021  
00022  
00023  
00024  
00025  
00026  
00027  
00028  
00029  
00030  
00031  
00032  
00033  
00034  
00035  
00036  
00037  
00038  
00039  
00040  
00041  
00042  
00043  
00044  
00045  
00046  
00047  
00048  
00049  
00050  
00051  
00052  
00053  
00054  
00055  
00056  
00057  
00058  
00059  
00060  
00061  
00062  
00063  
00064  
00065  
00066  
00067  
00068  
00069  
00070  
00071
```



```

00101
00102
00103
00104
00105
00106
00107
00108
00109
00110
00111
00112
00113
00114
00115
00116
00117
00118
00119
00120
00121
00122
00123
00124
10
20
30
40
50
60
70
80
90
100
110
120
130
140
150
SUBROUTINE MAXZ
C THIS ROUTINE USES THE POINTERS IN ARRAY J TO FIND THE MAXIMUM
C MAY EXCURSION OVER EACH CYCLE
COMMON/RESULT/Z1(1000),Z1(1000),Z1(1000),Z1(1000),Z1(1000),Z1(1000),
* J1(200),AV1(200),ZMAX1(200),ACT1(100),Z01(200),A1(200),N
1C=Z1(1000)-1
DO 10 I=1,LCN=1
K1(J1(I))
K2(J1(I))
TEMP=ABS(Z1(K1))
DO 20 K=1,K2
30 IF (ABS(Z1(K1)-Z1(K2)))GT.ABS(TEMP)-Z1(K))
10 ZMAX1(I)=TEMP
RETURN
END
00000
00001
00002
00003
00004
00005
00006
00007
00008
00009
00010
00011
00012
00013
00014
00015
00016
00017
00018
00019
00020
00021
00022
00023
00024

```

CASE 1  
 D= 1.000E-02 METERS  
 S= 1.1000E-01 \*  
 G= 0.351E-02 CHANNEL WIDTH GRADIENT  
 G= 0.2000 MZ (AZIAL SPEED GRADIENT IN RANGES)  
 C= 1.000E+00 W/SFC  
 A= 1.000E+00 M  
 Z= 3.637E-01 RADIAN OF 7.000E-01 DEGREES  
 Z= 0.0000  
 PROFILE: 1 (10M104CM, ZOPARADOLIC, J00LLINFA)

RESULTS:

MSMO 2 AT STEP 150

MSMO 3 AT STEP 1520

MAXIMUM DISTANCE AT STEP 1562

CHANNEL WIDTH LESS THAN 0.01 AT STEP 1562

AXIS CROSSINGS: 0

SUMMARY OF AXIS CROSSINGS:

NUMBER	STEP	RANGE	(M)	TIME	(SEC)	AXIS CROSSINGS	(M/SEC)	A/AO	MAX Z	(M)	W/40	(SEC)
1	1	0.00000	0.00000	0.00000	0.00000	0.00000	0.00000	1.00000E+00	3.26650E-01	2.67620E+00	1.89526E-01	
2	249	2.67620E+00	2.67620E+00	2.67620E+00	2.67620E+00	2.67620E+00	2.67620E+00	9.30030E-01	-2.97787E-01	2.19065E+00	1.83946E-01	
3	498	4.85951E+00	4.85951E+00	4.85951E+00	4.85951E+00	4.85951E+00	4.85951E+00	5.77051E-01	-2.71899E-01	1.79267E+00	1.83946E-01	
4	647	6.85951E+00	6.85951E+00	6.85951E+00	6.85951E+00	6.85951E+00	6.85951E+00	5.77051E-01	-2.71899E-01	1.79267E+00	1.83946E-01	
5	814	8.12596E+00	8.12596E+00	8.12596E+00	8.12596E+00	8.12596E+00	8.12596E+00	4.83922E-01	-2.71555E-01	1.19451E+00	1.83946E-01	
6	1053	9.32060E+00	9.32060E+00	9.32060E+00	9.32060E+00	9.32060E+00	9.32060E+00	4.08053E-01	-2.02717E-01	9.78630E+00	1.83946E-01	
7	1299	1.03001E+01	1.03001E+01	1.03001E+01	1.03001E+01	1.03001E+01	1.03001E+01	3.45840E-01	-1.93380E-01	7.98924E+00	1.83946E-01	
8	1408	1.10903E+01	1.10903E+01	1.10903E+01	1.10903E+01	1.10903E+01	1.10903E+01	2.95100E-01	-1.78936E-01	6.50157E+00	1.83946E-01	
9	1538	1.17491E+01	1.17491E+01	1.17491E+01	1.17491E+01	1.17491E+01	1.17491E+01	2.53801E-01	0.00000	0.00000	0.00000	

THIS PAGE IS BEST QUALITY FRAGILE  
 (10M104CM, ZOPARADOLIC, J00LLINFA)

CASE 2  
 D= 1.0000-02 METERS  
 WAKE 2.341700-01 "  
 GRAD1=3.1752-02 CHANNEL WIDTH GRADIENT  
 GRAD2= 0.0000 WY LATERAL SPEED GRADIENT IN RANGEL  
 CO= 1.0000-00 W/SEC  
 AC= 1.0000-00 "  
 ZONE 3.6397-01 RADIANS OR 2.0000-01 DEGREES  
 Z0= 0.0000 "  
 PROFILE: 1 11-HIRSCH, ZOBANRANOLIC, JOELLINARI

RESULTS:

MESH 2 AT STEP 1427

MESH 3 AT STEP 2952

MAXIMUM DISTANCE AT STEP 3295

CHANNEL WIDTH LESS THAN 0.01 AT STEP 3295

AXIS CROSSINGS: 16

SUMMARY OF AXIS CROSSINGS:

NUMBER	STEP	WAVE	WAVE	TIME	AVG(DR/DT)	AVD	MAX Z	SP/AD	J
				(SEC)	(M/SEC)		(M)		(SEC)
1	1	0.00000	0.00000	0.00000	9.97837-01	1.000000-00	3.341714-01	2.809510-00	3.683913-01
2	282	2.809510-00	2.815525-00	2.815525-00	9.973717-01	9.107269-01	-3.189649-01	2.542109-00	3.609492-01
3	617	5.351610-00	5.364276-00	5.364276-00	9.968119-01	8.300407-01	3.055518-01	2.300038-00	3.637702-01
4	747	7.651637-00	7.671653-00	7.671653-00	9.961209-01	7.570043-01	-2.908967-01	2.080086-00	3.607151-01
5	976	9.732692-00	9.760643-00	9.760643-00	9.952644-01	6.902337-01	2.779668-01	1.882468-00	3.678670-01
6	1193	1.161501-01	1.145207-01	1.145207-01	9.942219-01	6.311421-01	-2.657244-01	1.702908-00	3.677626-01
7	1333	1.331287-01	1.336477-01	1.336477-01	9.929464-01	5.770460-01	2.541486-01	1.590115-00	3.662567-01
8	1497	1.485793-01	1.491503-01	1.491503-01	9.913942-01	5.281566-01	-2.431976-01	1.392769-00	3.698338-01
9	1627	1.625070-01	1.632064-01	1.632064-01	9.886336-01	4.832644-01	2.379394-01	1.254086-00	2.190299-01
10	1877	1.750639-01	1.758979-01	1.758979-01	9.871947-01	4.440114-01	-2.231763-01	1.138731-00	1.827184-01
11	2104	1.844412-01	1.879329-01	1.879329-01	9.841914-01	4.070147-01	2.139698-01	1.029122-00	1.841937-01
12	2310	1.967374-01	1.978873-01	1.978873-01	9.807613-01	3.742369-01	-2.052928-01	9.297681-01	1.839959-01
13	2494	2.060301-01	2.073653-01	2.073653-01	9.768222-01	3.462102-01	1.971329-01	8.396776-01	1.840626-01
14	2644	2.144269-01	2.159613-01	2.159613-01	9.717774-01	3.194444-01	-1.894620-01	7.579539-01	1.849812-01
15	2814	2.220044-01	2.237610-01	2.237610-01	9.65452-01	2.944742-01	1.822616-01	6.837816-01	1.819176-01
16	2952	2.288492-01	2.308420-01	2.308420-01	9.587209-01	2.733594-01	-1.755462-01	6.140797-01	1.844666-01
17	3194	2.349450-01	2.372604-01	2.372604-01	0.000000	2.537582-01	0.000000	0.000000	0.000000

THIS PAGE IS BEST QUALITY PRACTICAL  
 FROM COPY FURNISHED TO DOD

CASE 3  
 DAB 1.0000-02 METERS  
 SHAR 3.542500-01 M  
 GRAB 1-2.1171-02 (CHANNEL WIDTH GRADIENT)  
 GRAB 2 0.0000 MZ (AZIAL SPEED GRADIENT IN RANGE)  
 COB 1.0000-00 M/SEC  
 AOB 1.0000-00 M  
 ZDAB 3.6347-01 RADIAN ON 1.9985-01 DEGREE  
 ZOB 0.0000 M  
 PROFILE: 1 (LUMINESCH, ZOPARABOLIC, PARILINEAR)

RESULTS:

RESMO 2 AT STEP 2102

RESMA 3 AT STEP 4362

MAXIMUM DISTANCE AT STEP 5204

CHANNEL WIDTH LESS THAN 0.01 AT STEP 5204

AXIS CROSSINGS: 24

SUMMARY OF AXIS CROSSINGS:

NUMBER	STEP	RANGE	TIME (SEC)	AVG (M/SEC)	A/R	MAX Z (M)	BP/AO	J (ISEC)
1	1	0.0000-00	0.000000	9.974911-01	1.000000-00	3.345031-01	2.856254-00	5.523896-01
2	247	7.866254-00	2.862144-00	9.974911-01	9.995303-01	-3.261921-01	2.872040-00	5.521909-01
3	554	5.523896-00	5.540399-00	9.971145-01	9.929401-01	3.142433-01	2.999693-00	5.509326-01
4	804	9.028004-00	8.034617-00	9.989371-01	8.900391-01	-3.046439-01	2.330308-00	5.524961-01
5	1038	1.028663-01	1.033249-01	9.984027-01	7.806331-01	2.973811-01	2.187434-00	5.518504-01
6	1267	1.255338-01	1.258740-01	9.980055-01	7.827229-01	-2.882993-01	2.046140-00	5.520455-01
7	1442	1.459999-01	1.464194-01	9.976439-01	6.909037-01	2.798350-01	1.913942-00	5.499095-01
8	1653	1.651339-01	1.654847-01	9.971956-01	6.503834-01	-2.715329-01	1.790195-00	5.533704-01
9	1832	1.830612-01	1.834473-01	9.968542-01	6.124833-01	2.638299-01	1.679370-00	5.016187-01
10	1999	1.997899-01	2.004842-01	9.932111-01	5.770353-01	-2.558178-01	1.565957-00	3.672142-01
11	2154	2.154445-01	2.162526-01	9.922448-01	5.438824-01	2.483741-01	1.444973-00	3.664184-01
12	2302	2.300693-01	2.310120-01	9.903814-01	5.124781-01	-2.412021-01	1.344723-00	3.674180-01
13	2475	2.473345-01	2.487917-01	9.878803-01	4.839855-01	2.343933-01	1.280748-00	3.673859-01
14	2631	2.645441-01	2.657730-01	9.844490-01	4.568704-01	-2.277464-01	1.197481-00	3.693153-01
15	3071	2.685190-01	2.698951-01	9.802151-01	4.315145-01	2.213874-01	1.119499-00	3.654794-01
16	3294	2.797139-01	2.811894-01	9.809545-01	4.078177-01	-2.152551-01	1.046961-00	3.675425-01
17	3504	2.901176-01	2.918141-01	9.824321-01	3.854631-01	2.093588-01	9.780591-00	2.974690-01
18	3700	2.999591-01	3.017455-01	9.804124-01	3.649544-01	-2.034980-01	9.139840-01	1.894097-01
19	3843	3.090990-01	3.110480-01	9.774400-01	3.454044-01	1.982544-01	8.539577-01	1.819044-01
20	4053	3.174384-01	3.198227-01	9.745104-01	3.275275-01	-1.930389-01	7.876823-01	1.894395-01
21	4213	3.254154-01	3.280081-01	9.704251-01	3.104397-01	1.882383-01	7.499570-01	1.834303-01
22	4342	3.330649-01	3.356408-01	9.654879-01	2.940883-01	-1.833751-01	6.931014-01	1.832884-01
23	4634	3.399954-01	3.428488-01	9.621902-01	2.801866-01	1.784803-01	6.492810-01	1.824662-01
24	4894	3.444884-01	3.496044-01	9.564389-01	2.644491-01	-1.742833-01	6.057944-01	1.844954-01
25	5141	3.575445-01	3.559371-01	9.000000	2.534238-01	0.000000	0.000000	0.000000

CASE N  
 DRY 1.0000-02 METERS  
 WBASE 4.723000-01 M  
 GRAD1=1.6400-02 CHANNEL WIDTH GRADIENT1  
 GRAD2=0.0000 MZ LATERAL SPEED GRADIENT IN RANGES  
 COE 1.0000-00 W/SEC  
 ADX 1.0000-00 W  
 ZDPRG 3.6497-01 RADIANS OR 2.0000-01 DEGREES  
 ZOE 0.0000 W  
 PROFILE: 1 LINEAR, 2 PARABOLIC, 3 BILINEAR

RESULTS:

WFSHO 2 AT STEP 2973

WFSHO 3 AT STEP 5910

MAXIMUM DISTANCE AT STEP 703

CHANNEL WIDTH LESS THAN 0.01 AT STEP 703

AXIS CROSSINGS: 32

Summary Of Axis Crossings:

Number	Step	WAVE	WAVE	TIME	TIME	AVG	AVG	MAX Z	EP/40	J
				(SEC)	(SEC)	(M/SEC)	(M/SEC)	(M)		(SEC)
1	1	0.0000	0.0000	0.0000	0.0000	0.0000	0.0000	3.380538-01	2.879400-00	7.361992-01
2	244	2.879400-00	2.885564-00	2.885564-00	2.885564-00	0.075790-01	0.075790-01	-3.302968-01	2.739168-00	7.360048-01
3	543	0.618768-00	0.630782-00	0.630782-00	0.630782-00	0.074240-01	0.074240-01	3.125437-01	2.605556-00	7.353405-01
4	874	0.224328-00	0.228070-00	0.228070-00	0.228070-00	0.063937-01	0.063937-01	3.152400-01	2.478931-00	7.365326-01
5	1072	1.070274-01	1.072803-01	1.072803-01	1.072803-01	0.066800-01	0.066800-01	3.080383-01	2.357477-00	7.360657-01
6	1308	1.306402-01	1.309265-01	1.309265-01	1.309265-01	0.066633-01	0.066633-01	3.010253-01	2.292391-00	7.354789-01
7	1632	1.530262-01	1.534254-01	1.534254-01	1.534254-01	0.063168-01	0.063168-01	2.941982-01	2.132868-00	7.320075-01
8	1948	1.748351-01	1.748332-01	1.748332-01	1.748332-01	0.059320-01	0.059320-01	2.876557-01	2.028694-00	7.3374078-01
9	1948	1.948421-01	1.952030-01	1.952030-01	1.952030-01	0.050505-01	0.050505-01	2.810896-01	1.929551-00	5.855151-01
10	2141	2.139374-01	2.145854-01	2.145854-01	2.145854-01	0.050340-01	0.050340-01	-2.740344-01	1.835212-00	5.499594-01
11	2324	2.322897-01	2.330293-01	2.330293-01	2.330293-01	0.045138-01	0.045138-01	2.680854-01	1.745442-00	5.513654-01
12	2499	2.497491-01	2.505800-01	2.505800-01	2.505800-01	0.038368-01	0.038368-01	-2.627338-01	1.640017-00	5.514275-01
13	2665	2.663493-01	2.672814-01	2.672814-01	2.672814-01	0.033032-01	0.033032-01	2.564975-01	1.578724-00	5.515057-01
14	2823	2.821315-01	2.831751-01	2.831751-01	2.831751-01	0.024014-01	0.024014-01	-2.513203-01	1.501342-00	5.520049-01
15	2973	2.971451-01	2.983004-01	2.983004-01	2.983004-01	0.011094-01	0.011094-01	2.458863-01	1.427920-00	5.487552-01
16	3257	3.113743-01	3.124576-01	3.124576-01	3.124576-01	0.008540-01	0.008540-01	-2.404038-01	1.357819-00	5.519504-01
17	3529	3.249524-01	3.263594-01	3.263594-01	3.263594-01	0.008890-01	0.008890-01	2.353748-01	1.291086-00	4.311752-01
18	3787	3.374634-01	3.394010-01	3.394010-01	3.394010-01	0.008507-01	0.008507-01	-2.303759-01	1.227469-00	3.670572-01
19	4032	3.501394-01	3.518143-01	3.518143-01	3.518143-01	0.007994-01	0.007994-01	2.254950-01	1.167108-00	3.665907-01
20	4264	3.618113-01	3.634303-01	3.634303-01	3.634303-01	0.005307-01	0.005307-01	-2.207570-01	1.109672-00	3.685449-01
21	4489	3.729091-01	3.748786-01	3.748786-01	3.748786-01	0.005133-01	0.005133-01	2.161560-01	1.054918-00	3.674805-01
22	4699	3.834572-01	3.855849-01	3.855849-01	3.855849-01	0.003450-01	0.003450-01	-2.114849-01	1.002790-00	3.660637-01
23	4899	3.934851-01	3.957822-01	3.957822-01	3.957822-01	0.001888-01	0.001888-01	2.073557-01	9.531564-01	3.670460-01
24	5090	4.030142-01	4.054994-01	4.054994-01	4.054994-01	0.000023-01	0.000023-01	-2.031497-01	9.058900-01	3.680295-01
25	5271	4.120759-01	4.147333-01	4.147333-01	4.147333-01	0.000000-01	0.000000-01	1.990448-01	8.608907-01	2.632086-01
26	5453	4.206447-01	4.235366-01	4.235366-01	4.235366-01	0.000000-01	0.000000-01	-1.951063-01	8.180332-01	1.846756-01
27	5607	4.288450-01	4.319211-01	4.319211-01	4.319211-01	0.000000-01	0.000000-01	1.917999-01	7.772003-01	1.827943-01
28	5762	4.366371-01	4.399078-01	4.399078-01	4.399078-01	0.000000-01	0.000000-01	-1.875546-01	7.383175-01	1.846197-01
29	5910	4.440203-01	4.475164-01	4.475164-01	4.475164-01	0.000000-01	0.000000-01	1.839908-01	6.987948-01	1.831034-01
30	6184	4.510082-01	4.547507-01	4.547507-01	4.547507-01	0.000000-01	0.000000-01	-1.805044-01	6.659889-01	1.846182-01
31	6456	4.574481-01	4.616594-01	4.616594-01	4.616594-01	0.000000-01	0.000000-01	1.771344-01	6.323400-01	1.839003-01
32	6709	4.639915-01	4.682443-01	4.682443-01	4.682443-01	0.000000-01	0.000000-01	-1.738697-01	6.002660-01	1.836428-01
33	6949	4.699947-01	4.746734-01	4.746734-01	4.746734-01	0.000000-01	0.000000-01	0.000000	0.000000	0.000000

THIS PAGE IS BEST QUALITY FRAGMENTED  
 FROM COPY FURNISHED TO DDG





```

000229
000230
000231
000232
000233
000234
000235
000236
000237
000238
000239
000240
000241
000242
000243
000244
000245
000246
000247
000248
000249
000250
000251
000252
000253
000254
000255
000256
000257
000258
000259
000260
000261
000262
000263
000264
000265
000266
000267
000268
000269
000270
000271
000272
000273
000274
000275
000276
000277
000278
000279
000280
000281
000282
000283
000284
000285
000286
000287
000288
000289
000290
000291
000292
000293
000294
000295
000296
000297
000298
000299
000300
000301
000302
000303
000304
000305
000306
000307
000308
000309
000310
000311
000312
000313
000314
000315
000316
000317
000318
000319
000320
000321
000322
000323
000324
000325
000326
000327
000328
000329
000330
000331
000332
000333
000334
000335
000336
000337
000338
000339
000340
000341
000342
000343
000344
000345
000346
000347
000348
000349
000350
000351
000352
000353
000354
000355
000356
000357
000358
000359
000360
000361
000362
000363
000364
000365
000366
000367
000368
000369
000370
000371
000372
000373
000374
000375
000376
000377
000378
000379
000380
000381
000382
000383
000384
000385
000386
000387
000388
000389
000390
000391
000392
000393
000394
000395
000396
000397
000398
000399
000400
000401
000402
000403
000404
000405
000406
000407
000408
000409
000410
000411
000412
000413
000414
000415
000416
000417
000418
000419
000420
000421
000422
000423
000424
000425
000426
000427
000428
000429
000430
000431
000432
000433
000434
000435
000436
000437
000438
000439
000440
000441
000442
000443
000444
000445
000446
000447
000448
000449
000450
000451
000452
000453
000454
000455
000456
000457
000458
000459
000460
000461
000462
000463
000464
000465
000466
000467
000468
000469
000470
000471
000472
000473
000474
000475
000476
000477
000478
000479
000480
000481
000482
000483
000484
000485
000486
000487
000488
000489
000490
000491
000492
000493
000494
000495
000496
000497
000498
000499
000500
000501
000502
000503
000504
000505
000506
000507
000508
000509
000510
000511
000512
000513
000514
000515
000516
000517
000518
000519
000520
000521
000522
000523
000524
000525
000526
000527
000528
000529
000530
000531
000532
000533
000534
000535
000536
000537
000538
000539
000540
000541
000542
000543
000544
000545
000546
000547
000548
000549
000550
000551
000552
000553
000554
000555
000556
000557
000558
000559
000560
000561
000562
000563
000564
000565
000566
000567
000568
000569
000570
000571
000572
000573
000574
000575
000576
000577
000578
000579
000580
000581
000582
000583
000584
000585
000586
000587
000588
000589
000590
000591
000592
000593
000594
000595
000596
000597
000598
000599
000600
000601
000602
000603
000604
000605
000606
000607
000608
000609
000610
000611
000612
000613
000614
000615
000616
000617
000618
000619
000620
000621
000622
000623
000624
000625
000626
000627
000628
000629
000630
000631
000632
000633
000634
000635
000636
000637
000638
000639
000640
000641
000642
000643
000644
000645
000646
000647
000648
000649
000650
000651
000652
000653
000654
000655
000656
000657
000658
000659
000660
000661
000662
000663
000664
000665
000666
000667
000668
000669
000670
000671
000672
000673
000674
000675
000676
000677
000678
000679
000680
000681
000682
000683
000684
000685
000686
000687
000688
000689
000690
000691
000692
000693
000694
000695
000696
000697
000698
000699
000700
000701
000702
000703
000704
000705
000706
000707
000708
000709
000710
000711
000712
000713
000714
000715
000716
000717
000718
000719
000720
000721
000722
000723
000724
000725
000726
000727
000728
000729
000730
000731
000732
000733
000734
000735
000736
000737
000738
000739
000740
000741
000742
000743
000744
000745
000746
000747
000748
000749
000750
000751
000752
000753
000754
000755
000756
000757
000758
000759
000760
000761
000762
000763
000764
000765
000766
000767
000768
000769
000770
000771
000772
000773
000774
000775
000776
000777
000778
000779
000780
000781
000782
000783
000784
000785
000786
000787
000788
000789
000790
000791
000792
000793
000794
000795
000796
000797
000798
000799
000800
000801
000802
000803
000804
000805
000806
000807
000808
000809
000810
000811
000812
000813
000814
000815
000816
000817
000818
000819
000820
000821
000822
000823
000824
000825
000826
000827
000828
000829
000830
000831
000832
000833
000834
000835
000836
000837
000838
000839
000840
000841
000842
000843
000844
000845
000846
000847
000848
000849
000850
000851
000852
000853
000854
000855
000856
000857
000858
000859
000860
000861
000862
000863
000864
000865
000866
000867
000868
000869
000870
000871
000872
000873
000874
000875
000876
000877
000878
000879
000880
000881
000882
000883
000884
000885
000886
000887
000888
000889
000890
000891
000892
000893
000894
000895
000896
000897
000898
000899
000900
000901
000902
000903
000904
000905
000906
000907
000908
000909
000910
000911
000912
000913
000914
000915
000916
000917
000918
000919
000920
000921
000922
000923
000924
000925
000926
000927
000928
000929
000930
000931
000932
000933
000934
000935
000936
000937
000938
000939
000940
000941
000942
000943
000944
000945
000946
000947
000948
000949
000950
000951
000952
000953
000954
000955
000956
000957
000958
000959
000960
000961
000962
000963
000964
000965
000966
000967
000968
000969
000970
000971
000972
000973
000974
000975
000976
000977
000978
000979
000980
000981
000982
000983
000984
000985
000986
000987
000988
000989
000990
000991
000992
000993
000994
000995
000996
000997
000998
000999
001000

```

THIS PAGE IS BEST QUALITY PRACTICABLE  
FROM COPY FURNISHED TO DDC





0101 047.001

\*\*\*\*\* RUN CONSISTS OF 1 SUBS\*\*\*\*\*

\*\*\*\*\* STOP: NUMBER AT5 \*\*\*  
USED INPUT UNITS FOR THE SUB: 2 (1:0.0/SEC,2:01.01/SEC)

DEPTH(FT) (CFT/SEC)  
C-0000 4956.0  
200-00 4950.0  
250-00 4950.5  
300-00 4955.0  
500-00 4965.0  
750-00 4933.0  
1000-0 4920.0  
1500-0 4890.0  
1750-0 4877.0  
2000-0 4866.0  
2250-0 4859.0  
2500-0 4855.0  
2750-0 4856.0  
3000-0 4855.5  
4000-0 4866.0  
5000-0 4876.0  
7000-0 4890.0  
10000- 4967.0

INPUT PARAMETERS:  
DR. 1.00\*02 METERS  
INITIAL DEPTH= 1.00\*02 METERS  
MAX ALLOWED DEPTH= 2.00\*04 METERS

CASE NUMBER: 1  
INITIAL ANGLE= 3.00\*01 DEGREES  
INITIAL SURF SPEED= 1509.0\*00 M/SEC  
PREDICTED WATER SPEED= 1509.7\*00 M/SEC  
SUMMARY OF TRAJECTORY:

THIS PAGE IS BEST QUALITY AVAILABLE  
FROM COPY FURNISHED TO DOD

E	STEP(S)	TYPE(S)	TYPE(S)	TYPE(S)	CTP	A(S)	AVGSP
	(M)	(SEC)	(M)	(M)	(M/SEC)	(SEC)	(M/SEC)
1	2.460382+04	1.809187+01	3.153575+03	1.509699+03	2.943917-01	1.485139+03	
2	5.392742+04	3.430942+01	9.920532+01	1.509697+03	2.943915-01	1.485141+03	
3	8.097702+04	5.452495+01	3.153588+03	1.509699+03	2.943947-01	1.485143+03	
4	1.080326+05	7.274446+01	9.921595+01	1.509699+03	2.943973-01	0.000000	

CASE NUMBER: 2  
 INITIAL ANGLE= 1.00+00 DEGREES  
 INITIAL SOUND SPEED= 1509.6+00 M/SEC  
 PREDICTED VELOCITY SPEED= 1509.6+00 M/SEC

SUMMARY OF TRAJECTORY:

E	STEP(S)	TYPE(S)	TYPE(S)	TYPE(S)	CTP	A(S)	AVGSP
	(M)	(SEC)	(M)	(M)	(M/SEC)	(SEC)	(M/SEC)
1	2.448372+04	1.797124+01	3.143432+03	1.509872+03	2.984156-01	1.485134+03	
2	5.373410+04	3.418335+01	9.881870+01	1.509868+03	2.984402-01	1.485136+03	
3	8.078443+04	5.439939+01	3.143429+03	1.509872+03	2.984396-01	1.485139+03	
4	1.078348+05	7.261343+01	9.881995+01	1.509868+03	2.984396-01	0.000000	

CASE NUMBER: 3  
 INITIAL ANGLE= 1.50+00 DEGREES  
 INITIAL SOUND SPEED= 1509.6+00 M/SEC  
 PREDICTED VELOCITY SPEED= 1510.2+00 M/SEC

SUMMARY OF TRAJECTORY:

E	STEP(S)	TYPE(S)	TYPE(S)	TYPE(S)	CTP	A(S)	AVGSP
	(M)	(SEC)	(M)	(M)	(M/SEC)	(SEC)	(M/SEC)
1	2.452187+04	1.786407+01	3.179081+03	1.510159+03	3.017698-01	1.485127+03	
2	5.356446+04	3.407300+01	9.307384+01	1.510156+03	3.018507-01	1.485129+03	
3	8.060705+04	5.428192+01	3.179091+03	1.510159+03	3.018515-01	1.485131+03	
4	1.076496+05	7.249080+01	9.367809+01	1.510154+03	3.018516-01	0.000000	

CASE NUMBER: 4  
 INITIAL ANGLE= 2.00+00 DEGREES  
 INITIAL SOUND SPEED= 1509.6+00 M/SEC  
 PREDICTED VELOCITY SPEED= 1510.6+00 M/SEC

SUMMARY OF TRAJECTORY:

E	STEP(S)	TYPE(S)	TYPE(S)	TYPE(S)	CTP	A(S)	AVGSP
	(M)	(SEC)	(M)	(M)	(M/SEC)	(SEC)	(M/SEC)
1	2.438802+04	1.777545+01	3.202960+03	1.510582+03	3.044398-01	1.485128+03	
2	5.343107+04	3.598469+01	8.823454+01	1.510557+03	3.044298-01	1.485129+03	
3	8.047418+04	5.419305+01	3.202978+03	1.510582+03	3.044294-01	1.485132+03	
4	1.075173+05	7.240316+01	8.821079+01	1.510559+03	3.044303-01	0.000000	

CASE NUMBER: 5  
 INITIAL ANGLE= 2.50+00 DEGREES  
 INITIAL SOUND SPEED= 1509.6+00 M/SEC

THIS PAGE IS BEST QUALITY PRACTICABLE  
 NONE OBTAINED TO DDC

PREDICTED VERTER SPEED- 1517.1000 M/SEC

SUMMARY OF TRAJECTORY:

#	HTP(EN) (M)	HTP(EN) (SEC)	ZTP(EN) (M)	CTP (M/SEC)	JEN (SEC)	AVGSP (M/SEC)
1	2.62764+04	1.77090+01	3.23270+03	1.51108+03	3.12417+01	1.48522+03
2	5.34931+04	3.50894+01	6.74263+03	1.51107+03	3.12727+01	1.48523+03
3	8.05884+04	5.42702+01	3.21273+03	1.51108+03	3.12774+01	1.48523+03
4	1.07760+05	7.25509+01	8.74703+03	1.51107+03	3.12778+01	0.000000

CASE NUMBER: 6

INITIAL ANGLE- 3.00+00 DEGREES

INITIAL SOUND SPEED- 1509.4+00 M/SEC

PREDICTED VERTER SPEED- 1517.7+00 M/SEC

SUMMARY OF TRAJECTORY:

#	HTP(EN) (M)	HTP(EN) (SEC)	ZTP(EN) (M)	CTP (M/SEC)	JEN (SEC)	AVGSP (M/SEC)
1	2.42249+04	1.74674+01	3.24917+03	1.51171+03	3.19497+01	1.48705+03
2	5.55643+04	3.73989+01	2.98232+03	1.51102+03	3.21974+01	1.48704+03
3	8.48994+04	5.71243+01	3.24401+03	1.51177+03	3.21953+01	1.48764+03
4	1.14251+05	7.48493+01	1.49016+03	1.51092+03	3.22056+01	0.000000

CASE NUMBER: 7

INITIAL ANGLE- 3.50+00 DEGREES

INITIAL SOUND SPEED- 1509.4+00 M/SEC

PREDICTED VERTER SPEED- 1517.5+00 M/SEC

SUMMARY OF TRAJECTORY:

#	HTP(EN) (M)	HTP(EN) (SEC)	ZTP(EN) (M)	CTP (M/SEC)	JEN (SEC)	AVGSP (M/SEC)
1	2.42034+04	1.76534+01	3.31253+03	1.51243+03	3.28288+01	1.48621+03
2	5.43827+04	3.47487+01	5.96044+03	1.51092+03	3.31977+01	1.48621+03
3	8.29607+04	5.38419+01	3.31249+03	1.51246+03	3.31975+01	1.48621+03
4	1.11337+05	7.49353+01	1.49016+03	1.51092+03	3.31988+01	0.000000

CASE NUMBER: 8

INITIAL ANGLE- 4.00+00 DEGREES

INITIAL SOUND SPEED- 1509.4+00 M/SEC

PREDICTED VERTER SPEED- 1513.3+00 M/SEC

SUMMARY OF TRAJECTORY:

#	HTP(EN) (M)	HTP(EN) (SEC)	ZTP(EN) (M)	CTP (M/SEC)	JEN (SEC)	AVGSP (M/SEC)
1	2.42278+04	1.76692+01	3.36289+03	1.51328+03	3.38197+01	1.48583+03
2	5.41987+04	3.44944+01	5.96044+03	1.51092+03	3.42016+01	1.48583+03
3	8.21894+04	5.33194+01	3.34299+03	1.51330+03	3.42037+01	1.48584+03
4	1.10160+05	7.41444+01	2.98232+03	1.51092+03	3.42168+01	0.000000

THIS PAGE IS BEST QUALITY PRINTING  
FROM COPY FURNISHED TO DDC

CASE NUMBER: 9  
 INITIAL ANGLE= 4.50+00 DEGREES  
 INITIAL SOUND SPEED= 1509.6+00 M/SEC  
 PREDICTED VELOCITY SPEED= 1514.3+00 M/SEC

SUMMARY OF TRAJECTORY:

E	STEP(S)	TYPE(S)	ZP(S)	CTP	A(S)	AVGSP
(P)	(SEC)	(M)	(M/SEC)	(SEC)	(M/SEC)	
1	2.438248+04	1.771874+01	3.420929+03	1.514330+03	3.494449+01	1.485444+03
2	5.407807+04	3.641473+01	5.940644+08	1.510592+03	3.540134+01	1.485444+03
3	8.183333+04	5.511047+01	3.420849+03	1.514330+03	3.539415+01	1.485444+03
4	1.094283+05	7.380598+01	2.980232+08	1.510592+03	3.542401+01	0.000000

CASE NUMBER: 10  
 INITIAL ANGLE= 5.00+00 DEGREES  
 INITIAL SOUND SPEED= 1509.6+00 M/SEC  
 PREDICTED VELOCITY SPEED= 1515.4+00 M/SEC

SUMMARY OF TRAJECTORY:

E	STEP(S)	TYPE(S)	ZP(S)	CTP	A(S)	AVGSP
(M)	(SEC)	(M)	(M/SEC)	(SEC)	(M/SEC)	
1	2.443431+04	1.780576+01	3.483805+03	1.515408+03	3.420833+01	1.485384+03
2	5.415141+04	3.644313+01	5.940644+08	1.510592+03	3.474279+01	1.485384+03
3	8.184872+04	5.512062+01	3.480317+03	1.515426+03	3.471605+01	1.485384+03
4	1.095466+05	7.377804+01	5.940644+08	1.510592+03	3.474248+01	0.000000

CASE NUMBER: 11  
 INITIAL ANGLE= 5.50+00 DEGREES  
 INITIAL SOUND SPEED= 1509.6+00 M/SEC  
 PREDICTED VELOCITY SPEED= 1516.6+00 M/SEC

SUMMARY OF TRAJECTORY:

E	STEP(S)	TYPE(S)	ZP(S)	CTP	A(S)	AVGSP
(M)	(SEC)	(M)	(M/SEC)	(SEC)	(M/SEC)	
1	2.463200+04	1.793615+01	3.559167+03	1.516624+03	3.740934+01	1.485443+03
2	5.440374+04	3.642954+01	7.450581+08	1.510592+03	3.823949+01	1.485443+03
3	8.217827+04	5.532488+01	3.540904+03	1.514645+03	3.817219+01	1.485443+03
4	1.099526+05	7.401988+01	5.940644+08	1.510592+03	3.824834+01	0.000000

CASE NUMBER: 12  
 INITIAL ANGLE= 6.00+00 DEGREES  
 INITIAL SOUND SPEED= 1509.6+00 M/SEC  
 PREDICTED VELOCITY SPEED= 1518.6+00 M/SEC

SUMMARY OF TRAJECTORY:

E	STEP(S)	TYPE(S)	ZP(S)	CTP	A(S)	AVGSP
(M)	(SEC)	(M)	(M/SEC)	(SEC)	(M/SEC)	
1	2.490877+04	1.811854+01	3.644316+03	1.517957+03	3.915997+01	1.485426+03
2	5.484307+04	3.692042+01	5.940644+08	1.510592+03	3.983713+01	1.485426+03
3	8.278463+04	5.572441+01	3.642583+03	1.517974+03	3.978899+01	1.485426+03

4 1.107235-05 7.452780-01 7.980232-08 1.510392-03 3.987426-01 0.000000

CASE NUMBER: 13  
 INITIAL ANGLE= 0.50-00 DEG/SEC  
 INITIAL SOUND SPEED= 1509.4-06 M/SEC  
 PREDICTED VELOCITY SPEED= 1519.4-00 M/SEC

SUMMARY OF TRAJECTORY:

E	ZTP (M)	TTP (SEC)	ZTP (M)	CTP (M/SEC)	J (SEC)	AVGSP (M/SEC)
1	2.720314-04	1.834504-01	3.213400-03	1.510400-03	4.004403-01	1.484149-03
2	5.50280-04	3.733350-01	3.225298-03	1.510392-03	4.164387-01	1.484149-03
3	8.373116-04	5.634764-01	3.735040-03	1.510445-03	4.153763-01	1.484149-03
4	1.119588-05	7.534124-01	5.940444-03	1.510392-03	4.164510-01	0.000000

CASE NUMBER: 14  
 INITIAL ANGLE= 7.00-00 DEG/SEC  
 INITIAL SOUND SPEED= 1509.4-06 M/SEC  
 PREDICTED VELOCITY SPEED= 1521.6-00 M/SEC

SUMMARY OF TRAJECTORY:

E	ZTP (M)	TTP (SEC)	ZTP (M)	CTP (M/SEC)	J (SEC)	AVGSP (M/SEC)
1	2.778430-04	1.869473-01	3.836912-03	1.520979-03	4.273430-01	1.480645-03
2	5.42957-04	3.794315-01	5.960444-03	1.510392-03	4.354244-01	1.480645-03
3	8.507849-04	5.723391-01	3.817703-03	1.520991-03	4.345107-01	1.480645-03
4	1.132278-05	7.650490-01	5.940444-03	1.510392-03	4.350013-01	0.000000

CASE NUMBER: 15  
 INITIAL ANGLE= 7.50-00 DEG/SEC  
 INITIAL SOUND SPEED= 1509.4-06 M/SEC  
 PREDICTED VELOCITY SPEED= 1522.7-00 M/SEC

SUMMARY OF TRAJECTORY:

E	ZTP (M)	TTP (SEC)	ZTP (M)	CTP (M/SEC)	J (SEC)	AVGSP (M/SEC)
1	2.844094-04	1.913934-01	3.934112-03	1.522608-03	4.470307-01	1.487363-03
2	5.779047-04	3.801095-01	2.980232-03	1.510392-03	4.569604-01	1.487363-03
3	8.699285-04	5.849180-01	3.934938-03	1.522708-03	4.557374-01	1.487363-03
4	1.162672-05	7.817358-01	1.920933-03	1.510392-03	4.569643-01	0.000000

CASE NUMBER: 16  
 INITIAL ANGLE= 8.00-00 DEG/SEC  
 INITIAL SOUND SPEED= 1509.4-06 M/SEC  
 PREDICTED VELOCITY SPEED= 1524.5-00 M/SEC

SUMMARY OF TRAJECTORY:

E	ZTP (M)	TTP (SEC)	ZTP (M)	CTP (M/SEC)	J (SEC)	AVGSP (M/SEC)
1	2.911111-04	1.961111-01	4.011111-03	1.524444-03	4.561111-01	1.491111-03
2	5.822222-04	3.922222-01	3.022222-03	1.511111-03	4.652222-01	1.491111-03
3	8.733333-04	5.883333-01	4.033333-03	1.523333-03	4.643333-01	1.491111-03
4	1.164444-05	7.844444-01	2.044444-03	1.511111-03	4.654444-01	0.000000

1 2.940026+04 1.973585+01 4.000000+03 1.324477+03 4.783791-01 1.400405+03  
 2 5.954278+04 4.000780+01 5.940444-00 1.510392+03 4.799268-01 1.400421+03  
 3 8.969092+04 6.024650+01 4.090672+03 1.524499+03 4.788174-01 1.400426+03  
 4 1.190315+05 8.052591+01 3.940644-00 1.510392+03 4.861019-01 0.000000

CASE NUMBER: 17  
 INITIAL ANGLES= 0.50+00 DEG/SEC  
 INITIAL SOUND SPEED= 1500.4+00 M/SEC  
 PREDICTED WATER SPEED= 1520.4+00 M/SEC

SUMMARY OF TRAJECTORY:

E	STP(E)	TTP(E)	ZTP(E)	CTP	A(E)	AVGSP
(M)	(SEC)	(M)	(M/SEC)	(SEC)	(SEC)	(M/SEC)
1	3.070069+04	2.044665+01	4.240002+03	1.520400+03	4.953225-01	1.400049+03
2	6.227345+04	4.179740+01	1.192093-07	1.510392+03	5.051528-01	1.400044+03
3	9.374875+04	6.293570+01	4.258183+03	1.526422+03	3.843828-01	1.400049+03
4	1.253866+05	8.407380+01	1.192093-07	1.510392+03	5.854476-01	0.000000

CASE NUMBER: 18  
 INITIAL ANGLES= 0.50+00 DEG/SEC  
 INITIAL SOUND SPEED= 1500.4+00 M/SEC  
 PREDICTED WATER SPEED= 1520.5+00 M/SEC

SUMMARY OF TRAJECTORY:

E	STP(E)	TTP(E)	ZTP(E)	CTP	A(E)	AVGSP
(M)	(SEC)	(M)	(M/SEC)	(SEC)	(SEC)	(M/SEC)
1	3.154372+04	2.220770+01	4.450072+03	1.520400+03	5.233321-01	1.402442+03
2	6.402972+04	4.403217+01	3.940644-00	1.510392+03	5.343361-01	1.402509+03
3	1.007787+05	6.752674+01	4.454099+03	1.520400+03	5.328334-01	1.402516+03
4	1.340177+05	9.019722+01	2.900232-00	1.510392+03	5.350564-01	0.000000

CASE NUMBER: 19  
 INITIAL ANGLES= 0.50+00 DEG/SEC  
 INITIAL SOUND SPEED= 1500.4+00 M/SEC  
 PREDICTED WATER SPEED= 1530.4+00 M/SEC

SUMMARY OF TRAJECTORY:

E	STP(E)	TTP(E)	ZTP(E)	CTP	A(E)	AVGSP
(M)	(SEC)	(M)	(M/SEC)	(SEC)	(SEC)	(M/SEC)
1	3.954027+04	2.433900+01	4.744037+03	1.530433+03	5.563983-01	1.400253+03
2	7.049583+04	5.319050+01	1.192093-07	1.510392+03	5.679945-01	1.400260+03
3	1.190438+05	8.000120+01	4.742528+03	1.530433+03	5.669809-01	1.400271+03
4	1.600316+05	1.008090+02	3.940644-00	1.510392+03	5.682496-01	0.000000

CASE NUMBER: 20  
 INITIAL ANGLES= 0.50+01 DEG/SEC  
 INITIAL SOUND SPEED= 1500.4+00 M/SEC  
 PREDICTED WATER SPEED= 1532.4+00 M/SEC

MAX DEPTH EXCEEDS DEPTH LIMIT: 2.000000+04 METERS

## REFERENCES

1. D. E. Weston, Proc. Phys. Soc. (London) 73, 365-384 (1958).
2. R. C. Shockley, J. Acoust. Soc. Am. (to be published).
3. L. D. Landau and E. M. Lifshitz, *Mechanics*, Pergamon Press, Reading, Mass. pp 154-158 (1960).
4. D. M. Milder, J. Acoust. Soc. Am. 46, pp 1259-1263 (1969).
5. Byrd, PF and Friedman, MD, *Handbook of Elliptic Integrals for Engineers and Scientists*, Springer-Verlag, New York (1971).
6. Mathpac Univac Corporation. SPLN1 and SPLN2 are documented in a number of manuals covering resident subroutines.

**INITIAL DISTRIBUTION LIST**

**DEFENSE ADVANCED RESEARCH PROJECTS AGENCY  
DR. G. GUSTAFSON**

**ARPA RESEARCH CENTER  
MOFFETT FIELD, CA  
R. TRUEBLOOD**

**NAVAL ELECTRONIC SYSTEMS COMMAND  
PME-124 (CAPT H. COX)  
PME-124/60 (DR. G. HETLAND)  
NELEX-320 (CDR D. GRIFFITH)**

**NAVAL RESEARCH LABORATORY  
DR. B. ADAMS  
H. BROCK  
DR. B. HURDLE  
DR. R. FERRIS  
D. NUTILE  
A. GUTHRIE**

**NEW LONDON LABORATORY  
NAVAL UNDERWATER SYSTEMS CENTER  
CODE 314 (DR. H. WEINBERG)  
CODE 312 (DR. F. DI NAPOLI)**

**THE UNIVERSITY OF TEXAS  
APPLIED RESEARCH LABORATORY  
P.O. BOX 8029  
AUSTIN, TX 78712  
DR. L. HAMPTON  
DR. S. MITCHELL**

**BOLT BERANEK AND NEWMAN, INC.  
50 MOULTON STREET  
CAMBRIDGE, MA 02138  
DR. P. W. SMITH**

**INSTITUTE FOR ACOUSTICAL RESEARCH  
615 S.W. 2ND AVENUE  
MIAMI, FL 33130  
DR. W. JOBST  
L. DOMINIJANNI**

**OCEAN DATA SYSTEMS, INC.  
3581 KENYON STREET  
SAN DIEGO, CA 92110  
K. OSBORNE  
DR. F. RYAN  
DR. J. CROUCH**

**SCIENCE APPLICATIONS, INC.  
8400 WESTPARK DRIVE  
MC LEAN, VA 22101  
C. SPOFFARD**

**DEFENSE DOCUMENTATION CENTER (12)**